Sedimentation in the Gippsland Lakes as determined from sediment cores

Report to the Gippsland Coastal Board

Gary Hancock and Tim Pietsch

CSIRO Land and Water Science Report 40/06

June 2006

www.csiro.au

Sedimentation in the Gippsland Lakes as determined from sediment cores

Gary Hancock and Tim Piestch

CSIRO Land and Water

CSIRO Land and Water Science Report 40/06

June 2006

Acknowledgements

This work is funded by EPA Victoria, The State Government of Victoria (through the Gippsland Lakes Future Directions and Action Plan component of the Our Water –Our Future program), and CSIRO Land and Water. We thank Neil Biggins (EPA Victoria) and Danny Hunt (CSIRO Land and Water) for help with collection of the cores. Laboratory analyses were performed by Chris Leslie, Ken McMillan and Mark Raven (CSIRO Land and Water).

Executive Summary

Four sediment cores collected from the Gippsland Lakes have been examined to determine the rate and history of sediment accumulation. Two cores were collected from Lake Wellington, and one each from Lake King and Lake Victoria. Measurements were made of sediment porosity, major and trace element concentrations, and radionuclide activities. The fallout nuclides ^{210}Pb and ^{137}Cs were used to determine modern sedimentation rates (the last 100 years). Optical dating was undertaken on four sub-samples to determine longer-term accumulation rates.

Lake Wellington

Two cores were analysed from the central and centre-western regions of Lake Wellington. The cores show similar excess ^{210}Pb ($^{210}Pb_{ex}$) and ^{137}Cs profiles, with $^{210}Pb_{ex}$ being detected to a depth of around 24 cm, and ^{137}Cs to a depth of 22-24 cm. The profiles show that sediment in Lake Wellington is mixed to a depth of at least 10 cm. This surface mixed layer (SML) is mixed on a time scale which is rapid compared to the ^{210}Pb half-life (22 yrs). Below the SML the decay in excess ^{210}Pb is consistent with exponential decay, yielding a vertical accretion rate of around 0.23 ±0.02 cm yr^{-1}, or 1.05 kg m^{-2} yr^{-1}. This rate applies to the last 60-70 years, but due to the possibility of slow mixing below the SML it is considered an upper limit. When applied to the whole area of Lake Wellington a depositional load of 170 ±22 kt yr^{-1} is calculated.

Analysis of the fallout inventories of $^{210}Pb_{ex}$ provides a lower limit to sediment accumulation (122 ±12 kt yr^{-1}). The long-term (60-70 yr) depositional sediment load is therefore constrained lie in the range 110-192 kt yr^{-1}.

The geochemical composition of sediment delivered over the 60-70 years has changed, indicating a changing sediment source. This source change may indicate a different spatial source and/or erosion process, or it may reflect changing river hydrology (more energetic river flow).

Optical dating of deeper sediment in Lake Wellington (70-80 cm) and (122-128 cm) gave dates of 3500 ±500 and 4000 ±600 years. These dates equate to a mean long-term (pre-European settlement) accumulation rate of 0.025 ±0.004 cm yr^{-1}, or 0.115 ±0.018 kg m^{-2} yr^{-1}. The equivalent depositional load is 17 ±3 kt yr^{-1}, a value 6-10 times lower than load estimates for recent decades.

Lake Victoria and Lake King

The two cores from the eastern lakes were collected from the deepest water (~7 m depth). The sediment does not appear to be mixed, or if mixing is occurring it is slow compared to the accumulation rate. The excess ^{210}Pb profiles provide a chronology that, when calibrated using the first appearance of ^{137}Cs (1955), covers a period of 90-100 years. The cores from the two lakes provide long-term accumulation rates that are similar. The mean mass accumulation rate at the two sites over the last 30 years is ~3.5 kg m^{-2} yr^{-1}, which when applied to the entire areas of Lakes King and Victoria give a sediment load of 660 kt yr^{-1}. This load is nearly 10 times higher than the loads estimated using catchment modelling and river monitoring, and indicates that sediment is focussed in the deep water (~7 m) where the cores were taken. Thus these cores cannot be used to estimate absolute sediment loads being deposited in the eastern lakes.

A history of sediment accumulation has been constructed for the eastern Lakes which shows that, when averaged over a time of years-decades sediment accumulation has been relatively constant since the 1940's. The two cores gave different accumulation rate histories for the first part of the 1900's, suggesting a different spatial deposition pattern during this period.

Optical dating of sediment from the eastern lakes was inhibited by the lack of suitable grains, but corroborated the $^{210}Pb/^{137}Cs$ chronology by indicating the sediment age near the base of the cores is <150 years. It appears the cores in these lakes did not penetrate deep enough to access pre-European sediment.

Table of Contents

1. INTRODUCTION

1.1. Background

In November 2001 the CSIRO study of the biochemical function of the Gippsland Lakes was finalised (Webster et al., 2001). The report addressed the factors controlling water quality and algal blooms in the lakes, and identified the delivery of sediment and associated nutrients to the Gippsland Lakes as the major factor affecting the health of the lakes. The report estimated that a minimum 40% reduction in the load of sediment entering the lakes was required to substantially reduce the intensity of algal blooms. Following the CSIRO study a three year project investigating the major sources of sediment to the Gippsland Lakes was commenced in 2004. This project is due to be completed by October 2006, and is funded by the Gippsland Coastal Board and CSIRO Land and Water. The project aims to identify major erosion processes occurring in the landscape, and estimate sediment loads to the Gippsland Lakes.

The report described herein covers the methods and results of a discrete phase of the wider project, that of the history of sediment accumulation in the Gippsland Lakes. This phase of the project is funded by the Victorian Environmental Protection Agency, the Gippsland Coastal Board and CSIRO Land and Water.

1.2. Aims

It is anticipated that this study of sedimentation in the Lake will complement the sediment sourcing project by providing estimates of sediment accumulation rates, both pre- and post European. By comparing the geochemistry of the sediment profile as a function of sediment depth (time) it is anticipated that historical information on changing sediment and loads will be provided. There has been only one previous study of sedimentation in the basin of Lake Wellington (Reid, 1989), and this provided only a low resolution estimate of sediment accumulation. There are no known coring studies in Lake Victoria and Lake King.

The specific aims of this phase of the study are;

- determine sediment chronologies at selected sites in the Gippsland lakes
- determine changes in sedimentation rates over the past 100 years. In particular, compare sedimentation rates before and after European settlement.
- examine changes in sediment composition as a function of time, and if possible, relate these to catchment sediment sources

2. METHODS

2.1. Sample collection

Sediment cores were collected on 21-22 September 2004. The coring sites are shown in Figure 1. At each site a push-core (100 mm diameter and 0.75 m length) was collected, along with a longer PVC barrel core (80 mm diameter, 2 m length). The latter core was collected using a drop-hammer device and retrieved with a winch. The length of the sediment core was generally shorter than the tube or barrel length due to compression of the sediment. Coring was facilitated by a diver (N. Biggins) who collected the push-cores, and who ensured all PVC barrel cores entered the sediment vertically. The cores were kept upright at all times, and subsequently frozen within 12 hours of collection. The cores were kept frozen until required for analysis.

Core locations, lengths and visual descriptions are listed in Table 1. Photos of PVC and push cores are shown in Figures 2 and 3. Available funds allowed for the analysis of four cores. Those selected for analysis included two from Lake Wellington (LW2 and LW3), one from Lake King (LK1), and one from Lake Victoria (LV2).

2.2. Sample analysis

The cores were partially thawed in the laboratory and the sediment extruded and cut into horizontal depth sections ranging from 1 cm to 6 cm. Near-surface sections were sampled at smaller depth intervals. The depth sections were dried to determine the water content (porosity), and the dry sediment ground in a ring mill. Sediment sub-samples were taken for gamma and alpha spectroscopy, and x-ray fluorescence.

Gamma spectrometry was used for the determination of ^{226}Ra, ^{210}Pb and ^{137}Cs, and followed the methods of Murray et al. (1987). Briefly, the sediment was dried 50° C, ground in a ring mill and then cast in a polyester resin to form a disc of known geometry. The disc was counted for 1-2 days using intrinsic germanium gamma detectors. The detectors were calibrated using CANMET uranium ore BL-5, and thorium nitrate refined in 1906 (Amersham International).

Where ^{210}Pb activity was low (close to the ^{226}Ra activity) radiochemical separation and alpha spectrometry (Martin and Hancock, 2004) was used to give improved estimates of ^{210}Pb (via ^{210}Po analysis) for selected samples. This method involves the addition of a tracer isotope of known activity (^{209}Po supplied by Amersham, $\pm$1% uncertainty) to ~0.7 g of dry sediment. The sample was dissolved using strong acids, including HNO_3, HCl, HF and $HClO_4$. The polonium isotopes were then auto-plated onto a silver disc and analysed using high-resolution alpha spectrometry.

Major and trace element concentrations were determined using XRF analysis. Prior to analysis the sediment was washed free of interstitial salt by shaking it with demineralised water, centrifuging and decanting the supernatant. This process was repeated until less than 1% of the original salt remained. Major elements were fused in a lithium borate matrix (Norrish and Hutton, 1969). Trace elements were determined using the pressed powder method (Norrish and Chappell, 1977).

Sediment for optical dating was sub-sampled from the centre of the PVC cores under subdued light (red filter). Preparation involved the isolation of pure extracts of 180-212 μm light safe quartz grains from the centre of the cores and following standard procedures (e.g. Aitken, 1998). Treatments were applied to remove contaminant carbonates, feldspars, organics, heavy minerals and acid soluble fluorides. The outer ~10 μm alpha-irradiated rind of each grain was removed by double etching each sample in 48 % hydrofluoric acid.

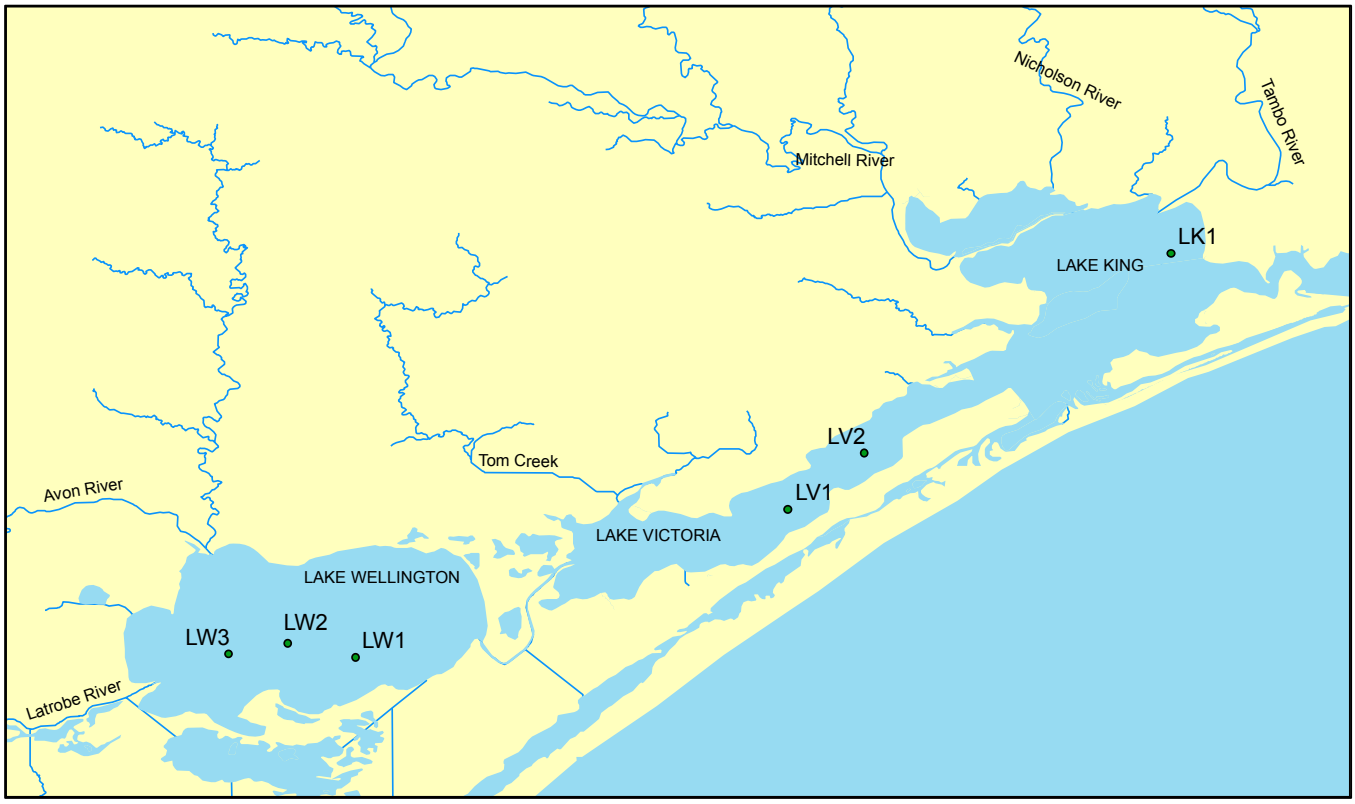

Figure 1. Location of coring sites

Figure 2. Collection of cores (80 mm diameter PVC).

Figure 3. (Left) 100 mm push-cores from Lake Wellington sites 1 and 2. (Right) close-up of a polycheate worm in core Lake Wellington site 3 (LW3/1). The burrowing activity of the worm appears to extend from 22 to 28 cm from the core surface.

Core	Location	Water depth	Core type, length	Description
Lake Wellington				
LW1/1	Central, deepest part of lake 38 06.300 S; 147 20.836E	3.6 m	Transparent poly-carb push-core, 100 diam. 48 cm length	0-2 cm light brown oxidised layer at surface. Dark brown below with darker layer at 12 cm Dark grey layer below 14 cm.
LW1/2	"	3.6 m	PVC, 50 mm diam 1.53 cm length	Opaque core barrel, not opened
LW2/1	Central, deepest part of lake 38 05.825 S; 147 18.558E	3.5 m	Transparent poly-carb push-core, 100 diam. 64 cm length	0-2 cm, light brown oxidised layer at surface. 2-48 cm, slate grey sediment 48-64 cm, lighter brown sediment at base
LW2/1	"	3.5 m	PVC, 50 mm diameter 1.28 cm length	Opaque core barrel, not opened
LW3/1	Most westerly site 38 06.190 S; 147 16.585E	3.1 m	Transparent poly-carb push-core, 100 diameter 63 cm length	0-6 cm light brown oxidised layer at surface. 6-42 cm: dark slate grey. 42-63 cm: lighter grey-brown.
LW3/2	"	3.1 m	PVC, 50 mm diameter 1.27 cm length	Opaque core barrel, not opened
Lake Victoria				
LV1/1	Most westerly site 38 01.363S; 147 35.293 E	5.4 m	Transparent poly-carb push-core, 100 diameter 46 cm length	Homogeneous dark sediment
LV1/2	"	5.4 m	PVC, 50 mm diameter 1.38 cm length	Opaque core barrel, not opened.
LV2/1	Central lake site 37 59.479S; 147 37.844E	7.2 m	Transparent poly-carb push-core, 100 diameter 69 cm length	0-3 cm light brown oxidised layer at surface. 2-66 cm: homogeneous dark sediment
LV2/2	"	7.2 m	PVC, 50 mm diameter 1.20 cm length	Opaque core barrel, not opened
Lake King				
LK1/1	Central lake site 37 52.801S; 147 48.107 E	6.6 m	Transparent poly-carb push-core, 100 diameter 69 cm length	Homogeneous dark sediment Shell fragments throughout
LK1/2	"	6.6 m	PVC, 50 mm diameter 1.20 cm length	Opaque core barrel, not opened

Table 1. Core descriptions

2.3. ^{210}Pb/^{137}Cs Geochronology

2.3.1. Origin of excess ^{210}Pb and ^{137}Cs

Sediment chronologies covering a time frame of up to 100 years were determined using the fallout radionuclides ^{210}Pb and ^{137}Cs. Naturally-occurring ^{210}Pb (half-life 22.3 y) is formed in the atmosphere by the decay of gaseous ^{222}Rn, and is deposited on the earth's surface by rainfall and dust. This results in the accumulation of "excess" ^{210}Pb in surface soils and sediments – the "excess" component being the difference between the ^{210}Pb and ^{226}Ra activities of the soil. As sediment accumulates and is buried in lakes and other water bodies excess ^{210}Pb ($^{210}Pb_{ex}$) decays towards the ^{226}Ra activity. Under favourable conditions the rate of sediment accumulation can be determined by the distribution of $^{210}Pb_{ex}$ in the sediment profile (Appleby and Oldfield, 1992). In the ideal situation where the sedimentation rate is approximately constant the decrease in the $^{210}Pb_{ex}$ as a function of sediment depth (x) will be approximately exponential, taking the form

$$y = C(0)e^{-bx} \qquad (1)$$

where $C(0)$ is the $^{210}Pb_{ex}$ at the sediment surface, and b is a constant. A least squares linear regression of a log-linear plot of $^{210}Pb_{ex}$ against depth yields a slope of -2.303b. The sedimentation rate (r) is determined from λ / b, where λ is the ^{210}Pb decay constant (0.031 yr^{-1}).

Anthropogenic ^{137}Cs occurs on the earth's surface as a result of fallout from atmospheric nuclear testing conducted mainly in the 1950's and 1960's. Fallout records indicate that ^{137}Cs first became detectable in Australian soil and sediments around 1955-58, the exact date depending on factors such as the sediment accumulation rate and the vertical thickness of sediment taken for analysis. For this work the first appearance of ^{137}Cs in the sediment record is assigned the date of 1955.

In constructing a chronology the sediment depth profiles of both excess ^{210}Pb and ^{137}Cs are considered in combination. The approach taken in this report is to apply conventional ^{210}Pb geochronological models to the depth distribution, and then assess how well the modelled chronology agrees with the first appearance of ^{137}Cs. Where the agreement is poor the model is then recalibrated using the 1955 ^{137}Cs horizon.

2.3.2. ^{210}Pb accumulation models

The two common approaches used to model the $^{210}Pb_{ex}$ distribution in sediments are the CIC (constant initial concentration) model and the CRS (constant rate of supply) model (Robbins, 1978; Appleby and Oldfield, 1992). The CIC model assumes the concentration (activity) of $^{210}Pb_{ex}$ attached to the depositing sediment particles has remained constant over the time frame of the chronology. The age (t) of sediment at depth i is calculated from

$$t_i = \frac{1}{\lambda} \ln \left[\frac{C(0)}{C(i)} \right]. \qquad (2)$$

When log $^{210}Pb_{ex}$ is plotted against depth (linear scale) the CIC approach allows linear segments of the curve to be analyses piece-wise, the slope of the linear segments (b in Equation 1) being used

to yield an estimate of sediment accumulation over the corresponding depth interval. The CIC approach fails when the decrease in excess ^{210}Pb activity with increasing depth is non-monotonic (i.e. it increases at some point in the profile). This event usually reflects a failure of the major assumption of CIC, that of constant $C(0)$. In profiles where this occurs the CRS approach is sometimes more appropriate. Using this model the age (t) of sediment at depth i is calculated from

$$t_i = -\frac{1}{\lambda}\ln\left[\frac{A(i)}{A(\infty)}\right] \quad (3)$$

where $A(i)$ is the integrated activity (Bq m^{-2}) of excess ^{210}Pb below depth i, and $A(\infty)$ is the total integrated activity of the sediment column, given by

$$A(\infty) = \sum_{i=1}^{\infty} c_i m_i \quad (4)$$

where c_i and m_i is the concentration and mass of the i^{th} depth interval. The CRS model assumes constant flux of ^{210}Pb$_{ex}$ to the sediment. The validity of this assumption depends on the mechanisms of sediment and ^{210}Pb delivery to the sediment accumulation zone of the water body. For both the CRS and CIC approaches verification of the calculated chronologies is required for confidence. As mentioned above ^{137}Cs is used for this purpose, with its first appearance in the mid-1950's providing an important mid-profile marker.

To model the ^{210}Pb$_{ex}$ distribution in mixed (bioturbated) sediment the two layer model (Robbins, 1978) is often employed. The 2-layer model, which is essentially a CIC model with a zero age off-set at the base of a surface mixed layer (SML), assumes that rapid mixing of sediment is occurring in the SML on a time scale short compared to the ^{210}Pb half-life (i.e. <22 years). The rapid mixing results in constant ^{210}Pb$_{ex}$ activities in the SML. Below the SML mixing is assumed absent. The vertical thickness of the SML is assumed to remain constant in time, and so as sediment is deposited the SML moves upward resulting in the transferral of sediment from the SML into the deeper layer. Thus the ^{210}Pb$_{ex}$ distribution in the deeper layer reflects a running average of sediment being delivered to the sediment surface, the time frame of this average being dependent on the thickness of the SML. The homogenising effect of the mixed layer can smooth out ^{210}Pb$_{ex}$ concentration variations resulting in a constant activity of ^{210}Pb$_{ex}$ being transferred to deeper sediment. For this reason a CIC analysis (a linear regression of the log-linear ^{210}Pb$_{ex}$-depth plot) can often be applied successfully to model ^{210}Pb$_{ex}$ distribution in the deeper layer.

2.4. Optical dating

Optical dating utilises the accumulation through time of trapped energy in crystalline materials such as quartz. When quartz grains are buried, they begin to accumulate a population of electrons and electron holes trapped between the valence and conduction bands in crystal defects. The trapped electrons and electron holes originate from atoms ionized by incoming radiation (α, β, γ, cosmic radiation), with measurement of the trapped charge population undertaken via laboratory eviction using either heat (thermoluminescence), or, as is the case for this work, using light. The latter is termed optically stimulated luminescence (OSL). Photons produced upon recombination of the released electrons with electron holes associated with luminescence centres are related in number

to the received ionizing radiation dose. Given chemical stability, the lithogenic dose rate is taken as constant over the burial period (Aitken, 1985), as the half-lives of the main parent nuclides concerned (^{238}U, ^{234}Th, ^{40}K) are many orders of magnitude longer than the practical range of luminescence dating.

Exposure to sunlight releases the light-sensitive trapped electrons, thereby resetting the luminescence signal; a process commonly referred to as 'bleaching'. The time elapsed since sediment grains were last exposed to sunlight can be determined by measuring the luminescence signal from a sample of sediment, determining the equivalent natural dose (D_e) in grays (Gy) that this represents, and estimating the rate of exposure (D_r) in Gy yr^{-1} of the grains to ionising radiation during burial (Huntley et al., 1985; Aitken, 1998). The burial age of a sample may be obtained from the following equation:

$$Burial\ Age = \frac{D_e}{D_r} \tag{5}$$

In this study equivalent doses (D_e) were determined using a modified single-aliquot regSAR protocol (Olley et al., 2004). A dose-response curve was constructed for each grain. Grains were rejected if they did not produce a measurable OSL signal in response to the 0.5 Gy test dose, had OSL decay curves that did not reach background after 1 s of laser stimulation, or produced natural OSL signals that did not intercept the regenerated dose-response curves ('Class 3' grains of Yoshida et al., 2000). For samples from Lake Wellington, where the grain recovery was sufficient to allow statistical analysis, the 'central age model' of Galbraith et. al. (1999) has been used to measure D_e distribution over-dispersion and to calculate a burial dose (D_b, the dose which all grains have received since burial) based on the central tendency of the data. Uncertainties have been calculated using computer software written specifically for OSL analysis (Analyst 3.1b). The uncertainties include counting statistics, curve fitting errors and a 2% uncertainty to accommodate the reproducibility with which the laser can be positioned.

Lithogenic radionuclide activity concentrations were determined using high-resolution gamma spectrometry (described above), with dose rates calculated using the conversion factors of Stokes et al. (2003). β-attenuation factors were taken from Mejdahl (1979). Cosmic dose rates were calculated from Prescott and Hutton (1994). Dose rates have been calculated using the as-measured water contents and the as-measured radionuclide concentration. The secular disequilibrium evident in the upper ^{238}U series chain for all samples is assumed to have persisted throughout the burial period.

3. RESULTS

3.1. Lake Wellington

3.1.1. Sediment characteristics

Both push cores displayed a light brown oxidised layer in the upper few cm. Below this layer about 40 cm of dark slate-grey sediment was seen. The bottom 20 cm of both cores (~50-70 cm depth) contained a lighter-grey-brown layer.

Plots of sediment porosity and depth for the cores from the central region of Lake Wellington (LW2 and LW3) are shown in Figure 4. In both cores porosity is initially high at the sediment surface (>0.8), decreases to a value of around 0.77 at a depth of about 20 cm, and then increases again reaching a maximum of ~0.82 (67 % water by weight) at around 30 cm. The porosity remains approximately constant below this depth.

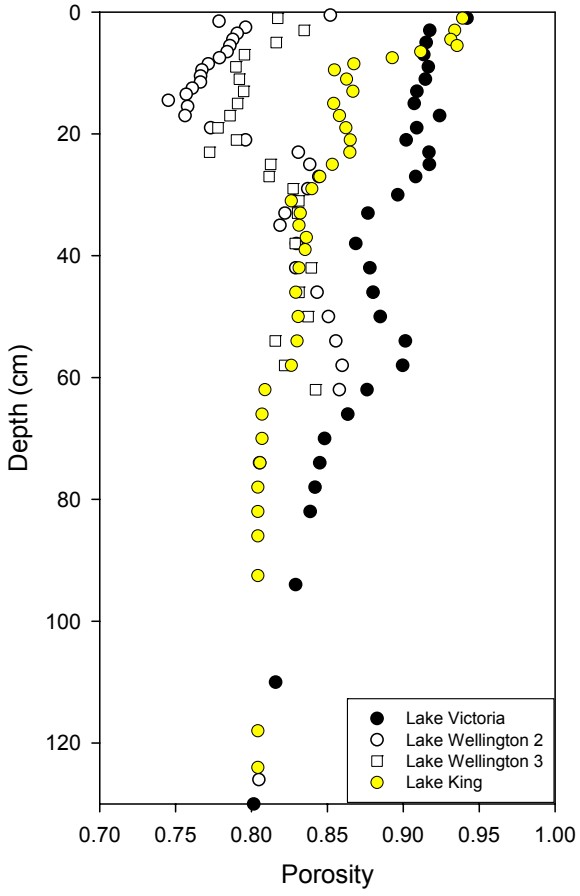

Figure 4. Sediment core porosities

Geochemical analysis shows that, for many oxides, a change occurs at about 22 cm depth (Figure 5). Major changes in the oxides of Si, Ti, Zr, Fe and P are seen, with Si, Ti, Zr and P decreasing below 22 cm, and Fe increasing. The organic component, as estimated by the weight loss on ignition at 450° C (LOI) increases slightly below 22 cm, but returns to surface values at around 40 cm.

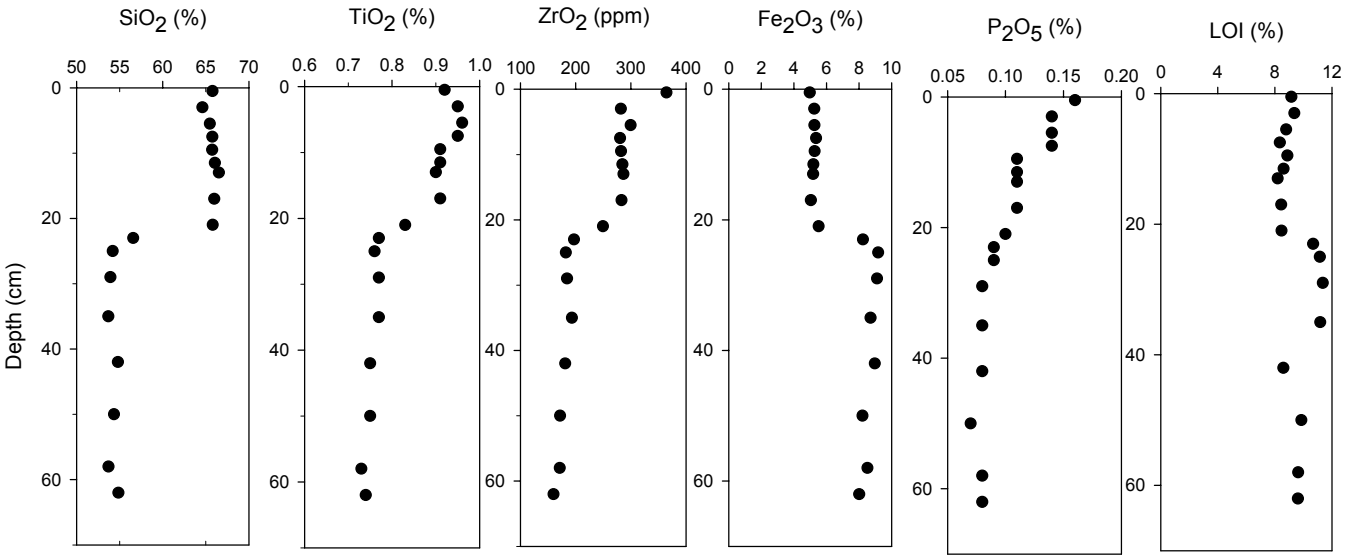

Figure 5. Oxide and LOI profiles for the LW2 core

3.1.2. Modern (^{210}Pb-^{137}Cs) chronology

The $^{210}Pb_{ex}$ and ^{137}Cs depth profiles of two cores from the central region of Lake Wellington are shown in Figure 6. The two cores show almost identical behaviour. The $^{210}Pb_{ex}$ activity is approximately constant in the upper 8-10 cm and declines in the region 8-24 cm. No $^{210}Pb_{ex}$ is detected below 22 cm in LW2/1 and 26 cm for LW3/1. We therefore apply the 2-layer model incorporating a surface mixed layer (SML), described above. For the two cores the mixing depths appear to be similar; 8 cm for LW2/1 and 10 cm for LW3/1. The linear regression of data in the layer immediately beneath the upper mixed layer gives apparent accumulation rates of 0.21 ±0.3 and 0.26 ±0.3 cm yr^{-1} (Figure 6). Conversion of these vertical accumulation rates to mass accumulation occurs by summing the accumulated mass over the relevant depth interval. The conversion is also well approximated by the relationship

$$r_m = r_l(1-\phi)\rho \qquad (6)$$

where r is the accumulation rate (cm yr^{-1}), and ϕ is the porosity below the SML (~0.78), ρ is the sediment dry density (2.3 g cm^{-3}). Equation 6 yields 1.07 ±0.16 kg m^{-2} yr^{-1} for LW2/1, and 1.26 ±0.12 kg m^{-2} yr^{-1} for LW3/1. Statistically these rates are not significantly different. Taking the average of these two rates (1.16 kg m^{-2} yr^{-1}) and applying it to the entire area of Lake Wellington (14.8 x 10^7 m^2) yields a sediment load of 172 ±18 kt yr^{-1}. This load is been averaged over the period of time corresponding to the decay profile of $^{210}Pb_{ex}$, i.e. 60-70 years.

The following important caveat should be noted regarding the above estimates of accumulation rates and sediment loads. Sediment mixing below the SML, albeit at a slower rate than within the SML, cannot be ruled out, and the accumulation rate and load estimates must therefore be considered upper limits. The presence of mixing below the SML is inferred from two lines of evidence; 1) the presence of a polychaete (burrowing worm) in LW3/1 at a depth of 22 cm (Figure 3); 2) the shape of the ^{137}Cs depth profile. Burrowing worms are likely to disturb sediment and the presence of one at 22 cm suggests that sediment disturbance is occurring to at least this depth. The ^{137}Cs profile also suggests that the sediment below the SML has been disturbed. ^{137}Cs activity is detectable to the 22-24 cm depth section of both cores. However, based on an accumulation rate of 0.20 cm yr^{-1} for LW2, and the assumed first appearance of ^{137}Cs in 1955, ^{137}Cs activity should not be seen lower than 10 cm below the mixed layer (ie. the 16-18 cm depth interval). Thus ^{137}Cs is seen about 6 cm deeper than it ought to be, a result consistent with mixing below the SML. For LW3 the first appearance of ^{137}Cs is calculated to be in the 20-22 m depth interval. Although the detection of ^{137}Cs in the 22-24 cm layer is only 2 cm lower than expected, a reasonable result given the sampling resolution and model assumptions, the similarity in the behaviour of ^{137}Cs and ^{210}Pb$_{ex}$ in both cores below 8 cm depth is also indicative of mixing. In Figure 6 the regression lines through ^{137}Cs and ^{210}Pb$_{ex}$ activities below the SML show that both ^{137}Cs and ^{210}Pb$_{ex}$ plots decrease in a similar way. Since ^{137}Cs delivery to surface sediments and soils can be considered a “once-off injection” over a finite period of time (~15 years) its decay profile is not expected to decrease in the same way as ^{210}Pb$_{ex}$, which is continually being deposited from the atmosphere. Their co-dependence below the SML indicates their concentrations are controlled by similar processes, such as physical transport in association with bioturbation.

As noted above, the possibility of mixing below the SML means that the sediment accumulation rates determined for LW2 and LW3 must be considered upper limits. Depending on the rate of mixing, the real accumulation rates and sediment loads could be considerably lower.

Table 2. Summary of parameters used to calculate modern (^{210}Pb$_{ex:}$ ^{137}Cs) accumulation rates for the two Lake Wellington cores.

Core	$C(0)$ (^{210}Pb$_{ex}$)	B	$r_{profile}$ (kg m^{-2} yr^{-1})	A_{∞}^{Pb} (Bq m^{-2})	A_{∞}^{Cs} (Bq m^{-2})	$r_{inventory}$ (kg m^{-2} yr^{-1})
LW2/1	47.3 ±3.1	0.156 ±0.024	1.07 ±0.16	2890 ±90	288 ±8	0.7 ±0.1
LW3/1	45.8 ±4.0	0.118 ±0.011	1.26 ±0.12	3320 ±130	277 ±10	1.1 ±0.2

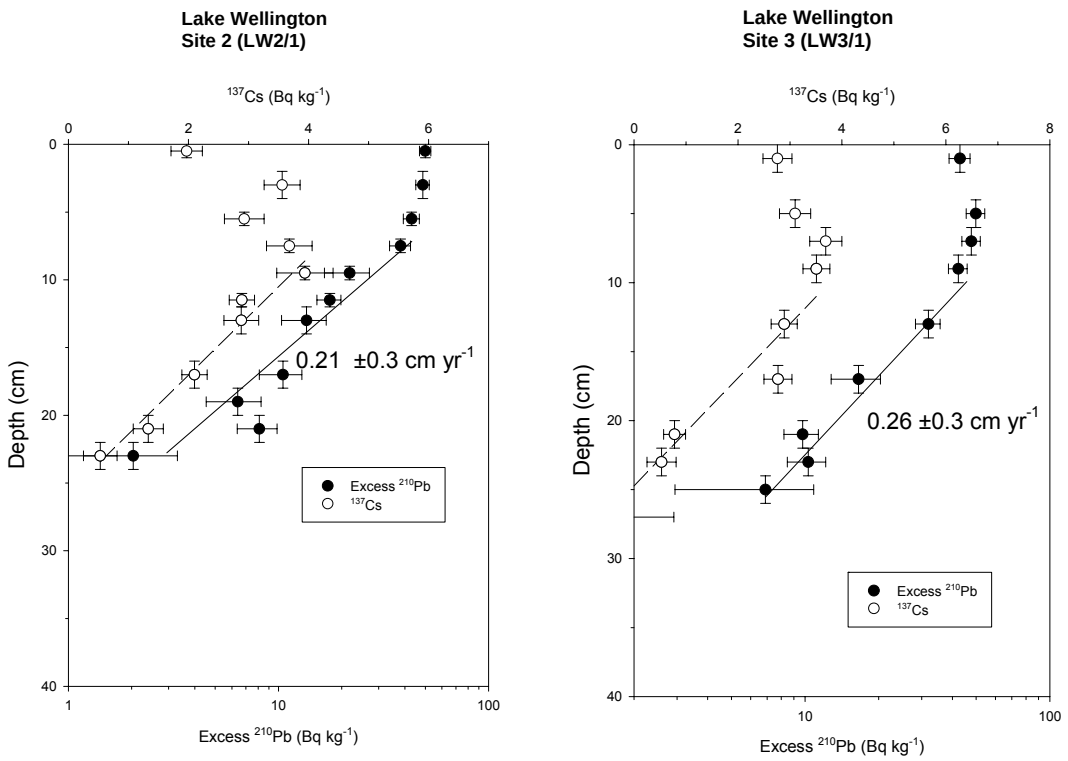

Figure 6. Lake Wellington core profiles. Note the log scale for $^{210}Pb_{ex}$. The linear segment below the surface mixed layer (upper 8-10 cm) gives the mean accumulation rate (cm yr^{-1}).

3.1.3. Core Inventories

Additional information can be obtained about sediment accumulation and movement within the Lakes by consideration of the total accumulated inventories of $^{210}Pb_{ex}$ and ^{137}Cs. Such an analysis provides a check on the accumulation rates determined using the exponential decay profile of $^{210}Pb_{ex}$ by comparing the amount of $^{210}Pb_{ex}$ seen in the sediment profile with the amount required to support the calculated accumulation rate. If the observed inventory is too low the accumulation rate determined from the $^{210}Pb_{ex}$ profile may be too high, possibly due to mixing below the SML.

The inventories are calculated by summing the activities of each nuclide over the entire depth range of the core, and are equivalent to $A(\infty)$ in Equation 4. The values of $A(\infty)$ for $^{210}Pb_{ex}$ (termed A_{∞}^{Pb}) and ^{137}Cs (A_{∞}^{Cs}) for the two Lake Wellington cores are given in Table 2. The values of A_{∞}^{Pb} at the two Lake Wellington sites are similar; 2880 ±90 Bq m^{-2} for LW2 and 3320 ±130 Bq m^{-2} for LW3. These measurements are higher than the value expected due to direct deposition of atmospheric ^{210}Pb, estimated to be 2100 Bq $m^{-2.}$ This latter value is determined from measured and literature values of fallout ^{210}Pb from areas of south-eastern Australia with similar mean annual rainfall to the Gippsland Lakes region (eg.Turekian et al., 1977; Wallbrink and Murray, 1996). The higher measured inventories in Lake Wellington is not surprising, given the Lake is not only receiving fallout ^{210}Pb directly from the atmosphere, but also $^{210}Pb_{ex}$ attached to sediment delivered from the catchment. For the LW2 core, the catchment component of the $^{210}Pb_{ex}$ inventory (A_{ct}^{Pb}), is given by the difference between the measured and expected inventories; i.e.

$$A_{ct}^{Pb} = A_{\infty}^{Pb} - A_{F}^{Pb} . \quad (7)$$

The value of A_{ct}^{Pb} is 730 ±90 Bq m^{-2}, equivalent to a $^{210}Pb_{ex}$ input rate of 24 ±3 Bq m^{-2} yr^{-1} (determined by dividing A_{ct}^{Pb} by λ, the ^{210}Pb decay constant). In other words, a mean annual rate of 24 Bq m^{-2} yr^{-1} of $^{210}Pb_{ex}$ must be delivered by sediment from the catchment, in addition to the direct fallout component, to account for the amount of $^{210}Pb_{ex}$ which has accumulated in the Lake sediment. Measurements of suspended and deposited sediment being delivered by Latrobe river water (below the town of Sale) during high river flow give an average ^{210}Pb value of ~ 76 Bq kg^{-1}, and an $^{210}Pb_{ex}$ value of 35 ±5 Bq kg^{-1}. Thus a sediment flux of 0.7 ±0.1 kg m^{-2} is required (24 Bq m^{-2} yr^{-1} divided by 35 Bq kg^{-1}). This value is ~35% lower than the accumulation rate estimated from the LW2 $^{210}Pb_{ex}$ profiles (1.05 kg m^{-2}). For LW3 the required catchment-derived $^{210}Pb_{ex}$ flux is 36 ±4 Bq kg^{-1}, yielding a depositional sediment flux of 1.1 ±0.2 kg m^{-2}, in good agreement with that estimated by the $^{210}Pb_{ex}$ profile (1.25 kg m^{-2}). The mean of the two estimates gives 0.83 ±0.12 kg m^{-2}, which when applied to the whole Lake yields a sediment load of 122 ±13 kt yr^{-1}.

It is emphasised that the estimation of sediment accumulation using $^{210}Pb_{ex}$ inventories is approximate, relying on recent measurements of ^{210}Pb in suspended sediment to represent longer-term (many decades) values of sediment bound ^{210}Pb. It also relies on transfer of 100% of the atmospheric fallout component of ^{210}Pb through the water column and into bottom sediments. If some of the direct fallout component of the ^{210}Pb budget (A_F) is lost from the lake through (for example) export to Lake Victoria, the inventory-based estimate of sediment load will be too low. Analysis of the ^{137}Cs core inventories indicates that some loss of sediment (and hence $^{210}Pb_{ex}$) from Lake Wellington may have occurred. The ^{137}Cs inventories measured in the two cores were almost identical (280 ±10 Bq m^{-2}). This value is 35% lower than the value expected from direct fallout (430 Bq m^{-2}, when decay-corrected to the year 2005). And given the fact that catchment input would have delivered additional ^{137}Cs from the catchment over the 50 year period since ^{137}Cs fallout commenced, (perhaps as much as 100 Bq m^{-2}), the amount of ^{137}Cs exported from the Lake may well be significantly greater than 35%. This export is presumably driven by tidal excursions and freshwater inflow to Lake Wellington. At face value the low ^{137}Cs inventory suggests that a similar amount of fallout ^{210}Pb may also have been lost, invalidating our $^{210}Pb_{ex}$ inventory-based calculation of sediment accumulation. However, due to the different chemistries of Cs and Pb it is not necessarily true that Pb is exported at the same rate as Cs. Differential behaviour of ^{137}Cs and ^{210}Pb in Lake Victoria and Lake King is noted and discussed in the next section, and is attributed to the greater solubility of ^{137}Cs compared to ^{210}Pb. This difference in solubility is likely to be significant in saline water where isotopic exchange of fallout ^{137}Cs with a large reservoir of stable dissolved Cs would enhance its solubility. Thus it is possible that fallout ^{137}Cs deposited directly to the lakes mainly in the dissolved form would remain in solution longer than fallout ^{210}Pb, allowing it to be exported to Lake Victoria rather than being scavenged by sediment and deposited in Lake Wellington.

The above analysis showing loss of ^{137}Cs (and possibly ^{210}Pb) from Lake Wellington indicates that the inventory-based estimate of sediment accumulation should be considered a lower limit. Thus the sediment load accumulating in Lake Wellington is constrained to lie between the uncertainty limits determined by the two methods; ie. 110-190 kt yr^{-1}. If 35% of the input load to Lake Wellington is being exported the input load is calculated to lie in the range 170-292 kt yr^{-1}. These estimates pertain to a period corresponding to approximately three ^{210}Pb half-lives (the last 60-70 years).

3.1.4. Optical dating; pre-European sedimentation rates

The results of OSL dating of Lake Wellington sediment are given in Table 3. The two samples extracted from the LW2 core (70-80 cm and 122-128 cm) have excellent luminescence characteristics, with over-dispersion parameters of 12% indicating that the sediments were well bleached prior to deposition. Radial plots of D_e populations for the Lake Wellington samples are shown in Figure 7. The measured D_e (in Gy) for a grain can be read by tracing a line from the *y*-axis origin through the point until the line intersects the radial axis (log scale) on the right-hand side. The corresponding standard error for this estimate can be read by extending a line vertically to intersect the *x*-axis. The *x*-axis has two scales: one plots the relative standard error of the D_e estimate (in %) and the other ('Precision') plots the reciprocal standard error. Therefore, values with the highest precisions and the smallest relative errors plot closest to the radial axis on the right of the diagram, and the least precise estimates plot furthest to the left. The shaded regions in the plots of Figure 7 indicate those D_e values that, at the 2σ confidence interval, are consistent with a single estimated burial dose as measured using the central age model.

Table 3. OSL dating results

Core	Depth (cm)	Number of Grains	D_e (Gy)	σ_d (%)	Age (yrs)
LW2/2	70-80	164	4.75 ±0.06	12	3500 ±500
LW2/2	122-128	110	5.46 ±0.08	12	4000 ±600
LK1/2	90-96	4	0.03±0.08	na	< 100
LK1/2	120-126	7	0.12±0.06	na	< 150
LV2/2	126-134	2	0.08±0.08	na	< 150

na; result not applicable due to insufficient number of grains

Given the uncertainties of measurement (~ ±20%) the two dates given in Table 2 are not significantly different; i.e. the constraints given by the uncertainty of the date for the 70-80 cm interval (3500 ±500 yr) overlap with the date for 122-128 cm (4000 ±600 yr). To calculate pre-European accumulation rates we assume that approximately 10 cm of sediment has accumulated over the last 100 years of European settlement. Although this estimate may be wrong by as much as ±50% it does not greatly affect the long-term accumulation rate calculations. The long term accumulation rates (cm yr^{-1}) are calculated from

$$\text{(OSL depth – 10 cm)/(OSL age – 100 yr)} \qquad (8)$$

where the OSL depth is taken as the midpoint of the depth section. The calculated rates are 0.019 ±0.03 cm yr^{-1} for the 70-80 cm interval, and 0.029 ±0.04 cm yr^{-1} for 122-128 cm (Table 2). These two rates straddle the long-term rate determined by Reid (1989) using a single radiocarbon measurement. Using the same rationale expressed in Equation 8, Reid's radiocarbon age of 3300 yr (no uncertainty available) for the 90-97 cm depth interval yields an accumulation rate of 0.026 cm yr^{-1}.

The average of the three pre-European accumulation rates determined by OSL and Reid is 0.025 ±0.004 cm yr^{-1}. Using a sediment porosity equal to 0.80 and a sediment dry density to 2.3 g cm^{-3} a

pre-European mass accumulation rate of 0.115 kg m^{-2} yr^{-1} is calculated. The lake-wide depositional load is 17 ±3 kt yr^{-1}. This is between 6 and 10 times lower than estimates of post-European loads to the Lake.

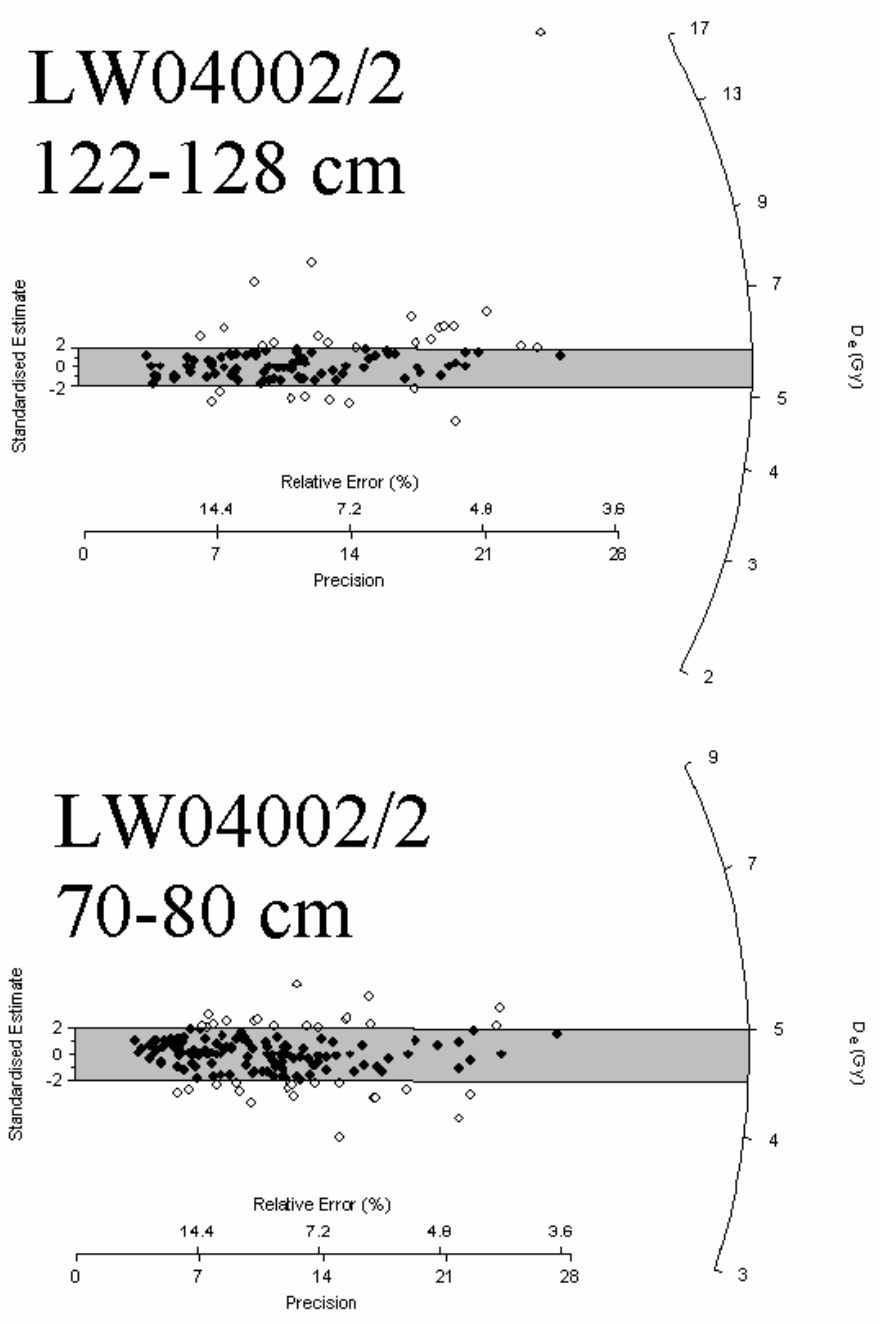

Figure 7. Radial plots of D_e populations for the Lake Wellington samples. The shaded regions in the plots of Figure indicate those D_e values that, at the 2σ confidence interval, are consistent with a single estimated burial dose as measured using the central age model.

3.2. Lake Victoria

3.2.1. Sediment characteristics

The Lake Victoria core LV2 is highly porous throughout, ranging from 0.94 at the surface to 0.80 at its base. The sediment was dark grey to black, with no visual change with depth. Geochemical profiles also showed little or no change with depth apart from elevated levels of P in the upper 6 cm. This high P is correlated with LOI, and hence the additional P is probably mostly associated with organic matter.

3.2.2. ^{210}Pb-^{137}Cs chronology

Excess ^{210}Pb (log scale) and ^{137}Cs depth profiles for Lake Victoria (site LV2) are shown in Figure 8. The decrease of $^{210}Pb_{ex}$ against depth can be interpreted as being essentially monotonic, with periods of linearity. The region of overlap between the short push-core core LV2/1 and the longer piston PVC core LV2/2 occurs at around 72 cm. Correlation between the two cores was good, and was checked using the ^{137}Cs profile. The offset between the two cores was just 2 cm, and the depths of the longer core were adjusted accordingly.

As was the case for Lake Wellington, modelling the distribution of $^{210}Pb_{ex}$ and ^{137}Cs raises the question of mixing of the upper sediment layer. However, in this case the exponential decline seen in the upper 10-12 cm indicates that mixing is either absent, or it is occurring at a rate slow compared to the ^{210}Pb half-life. In Figure 8 the slope of the linear regression through the upper-most linear interval yields an apparent accumulation rate of 0.54 cm yr^{-1}. If mixing was occurring near the surface elevated apparent accumulation rates would be expected. However, compared with deeper sediment, where mixing is almost certainly absent, a rate of 0.54 cm yr^{-1} is not high. For example, the apparent accumulation rate in the 22-50 cm interval is 0.91 cm yr^{-1}, and above and below the 22-50 cm interval approximately constant $^{210}Pb_{ex}$ activities are seen in the 12-22 cm and 70-70 cm depth ranges indicating extremely rapid accumulation. A lack of mixing in surficial sediment is not surprising in Lake Victoria, given the location of this core site in the deepest part of the lake (water depth ~7 m). This region is known to become thermally stratified and is likely to have low oxygen levels (Webster et al., 2001), limiting the activities of polychaete worms and other bioturbators.

^{137}Cs activity first appears in the 72-76 cm interval. Based on the high ^{137}Cs activities shown in this core, and the fact that the activity of the 72-76 interval (2.9 ±0.4 Bq kg^{-1}) is well above the ^{137}Cs detection limit, the earliest year of the onset period (1955-1958) is ascribed to the base of this interval i.e. 76 cm = 1955. The ^{137}Cs activity peaks at 12.4 Bq kg^{-1} in the 56-64 cm depth interval. It is likely this peak corresponds to, or post-dates the historical peak in ^{137}Cs fallout, which reached its maximum around 1964. We therefore ascribe the date 1965 to the base of peak activity depth interval; i.e., 1965 = 64 cm. The ^{137}Cs core profile does not mirror the decline exhibited by the fallout history over the last thirty years, where ^{137}Cs fallout has declined to almost zero. Rather, the profile in the upper 20-30 cm shows relatively constant ^{137}Cs activities around 5 Bg kg^{-1}. This is due to the fact that, in addition to direct atmospheric fallout during 1950's to 1970's, ^{137}Cs bound to sediment eroded from the lakes catchment has been delivered continuously to the Gippsland Lakes since 1975, the approximate date fallout ceased to be significant. Thus, in the absence of post-1975 fallout, the ^{137}Cs activity of sediment in the upper 20-30 cm of the core profile simply reflects the activity of catchment-derived sediment. Lake King (see below) shows similar ^{137}Cs activity for recent sediment deposition.

Assuming no post-depositional mixing of sediment, the CIC and CRS models have been applied to LV2 giving the age vs depth plots shown in Figure 8. Theoretically, the CIC model is not applicable at some points in the profile because the $^{210}Pb_{ex}$ activities fluctuate in accordance with their measurement error such that the $^{210}Pb_{ex}$ profile sometimes shows an increase with increasing depth thereby yielding ages at some depths which are younger than overlying sediment. However, despite these perturbations, the CIC approach can provide a constraint on sediment ages, providing a useful check on older CRS dates. The CIC model (closed circles, Figure 8) is clearly in error in recent decades because it produces ages which are not consistent with the ^{137}Cs markers; the CIC ages being about 20-30 years too old for the period 1965-1955. The CRS chronology (open circles) provides better estimates, although there is still an offset of about +6 years with the ^{137}Cs markers. To correct for this offset the 1955 ^{137}Cs marker is used to calibrate the $^{210}Pb_{ex}$ supply for the period 1955 to 2004. This is done using the approach of Appleby (2001), whereby constant $^{210}Pb_{ex}$ flux (F) is assumed between two horizons of known age; the known horizons being 1955 at 76 cm (t_1) and 2004 at depth 0 cm (t_2); ie.

$$F = \frac{\lambda A(t_1, t_2)}{e^{-\lambda t_1} - e^{-\lambda t_2}} \qquad (9)$$

where $A(t_1, t_2)$ is the $^{210}Pb_{ex}$ inventory between t_1 and t_2, corresponding to depths x_1 and x_2. The sediment age (t) at depth x is given by

$$t = \frac{1}{\lambda} \ln\left(e^{-\lambda t_1} + \frac{\lambda}{F} A(x, x_1) \right) \qquad (10)$$

where $A(x, x_1)$ is the $^{210}Pb_{ex}$ inventory between depth x and x_2. For this work, the $^{210}Pb_{ex}$ flux F is also assumed to apply to the decades preceding the 1950's. The chronology determined from Equation 10, termed CRS2, is shown in Figure 8 (open squares). Equation 10 has "forced" the CRS2 chronology through the 1955 ^{137}Cs marker; however good agreement is seen with the 1965 marker. The oldest horizon able to be dated using CRS2 is 98 ±4 yr (1906) at 108 cm. There is good agreement between CIC and CRS2 at this depth.

Using the CRS2 chronology, a history of sediment accumulation is constructed (Figure 9). The uncertainties in sediment ages are greatest for sediment older than 1950, and range from 2-6 years. This history should be taken as a guide only; the rates are likely to be correct on a decadal time scale, but analytical uncertainties and model inconsistencies, especially in the first half of the 20th century, could lead to errors greater than those indicated in Figure 9. The CRS2 chronology indicates that accumulation rates were relatively low in the first few decades of the 1900's. A peak in sediment deposition is seen in the period corresponding to the late 1940's through to the mid 1950's. Deposition rates are temporarily lower in the 1960's, increasing in the 1970's and 1980's. Sediment accumulation in the last 10-15 years appears to be similar to the long-term average. If 30 year averages are considered, the mean accumulation rate from 1918 to 1945 is 1.9 kg m^{-2} yr^{-1}, increasing to 4.0 kg m^{-2} yr^{-1} from 1945 to 1975. This latter rate has been maintained over the last 30 years. The long-term accumulation rate, averaged over the last 100 years, is 3.22 kg m^{-2} yr^{-1} (Table 4).

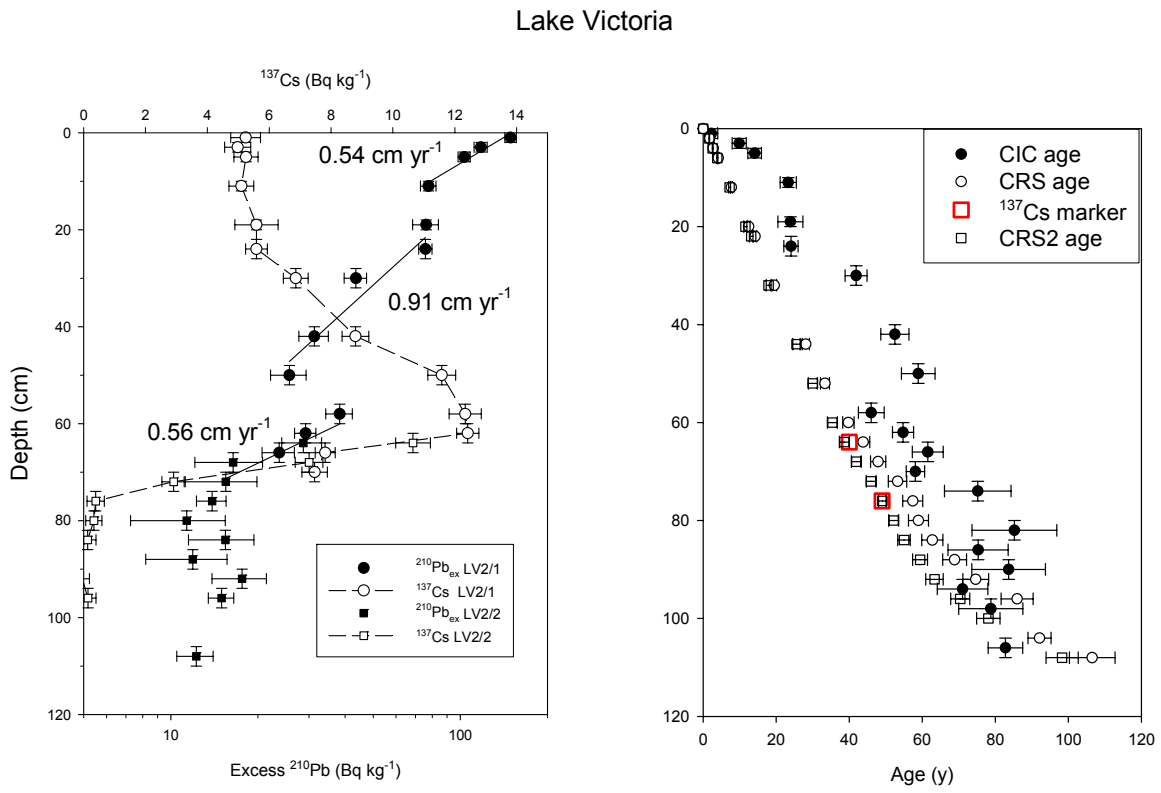

Figure 8. (Left) core profiles of $^{210}Pb_{ex}$ and ^{137}Cs for Lake Victoria. (Right) chronologies determined using the various models (see text for details). The chronology given by the (calibrated) CRS2 model has been adopted.

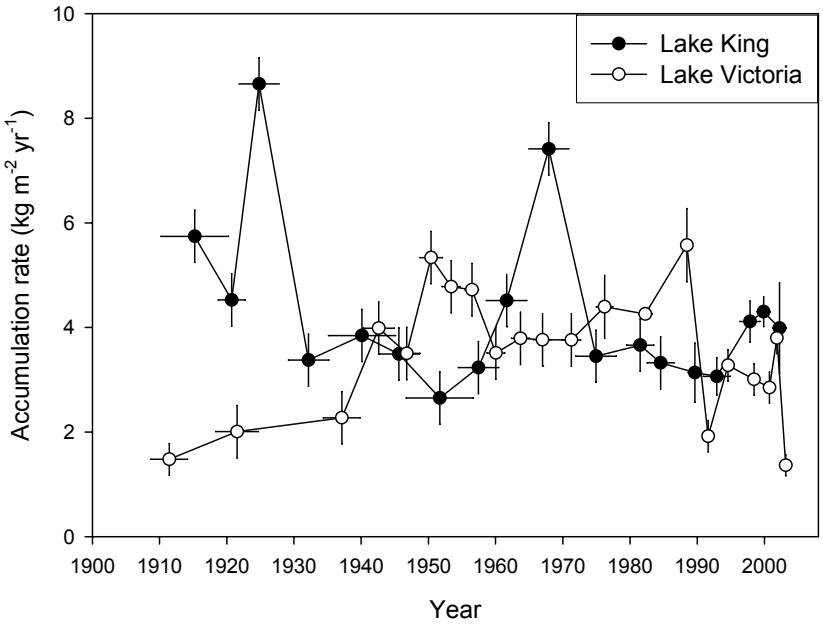

Figure 9. Sediment accumulation history in Lake Victoria and Lake King

3.3. Lake King

3.3.1. Sediment characteristics

The Lake King push-core core LK1/1 shows very high porosity at the surface (~0.92) decreasing with depth. The value at the base of the PVC core (128 cm depth) is about 0.80. Geochemical analysis indicates no significant trends.

3.3.2. ^{210}Pb-^{137}Cs chronology

Excess ^{210}Pb (log scale) and ^{137}Cs depth profiles for Lake King core #1 (LK2) are shown in Figure 10. As with Lake Victoria, the decrease of log $^{210}Pb_{ex}$ against depth is essentially monotonic, with periods of linearity. A surface layer section with approximately constant $^{210}Pb_{ex}$ activity occurs to a depth of 14 cm. The region of overlap between the short push-core core LK1/1 and the longer piston PVC core LK1/2 occurs at around 72 cm.

The ^{210}Pb chronology was initially assessed using a 2-layer mixing model, similar to Lake Wellington, with a SML of 14 cm. This produces an age versus depth profile shown in Figure 10. The agreement with the first appearance of ^{137}Cs is reasonable, although the scatter in ages (due to analytical uncertainties) is large below 40 cm depth. Also shown in Figure 10 is the calibrated CRS2 chronology; the ages were calculated in a similar fashion to Lake Victoria using the first appearance ^{137}Cs horizon at 52 cm to calibrate $^{210}Pb_{ex}$ supply, and assumes no mixed layer. Below 14 cm, the depth of the layer of constant $^{210}Pb_{ex}$ activity, the general agreement between the two models is good. In the sections below we show that the Lake Victoria and Lake King profiles of ^{137}Cs and $^{210}Pb_{ex}$ indicate similar long-term deposition rates. It is therefore assumed that surface layer mixing is absent in Lake King, as it appears to be in Lake Victoria, and the CRS2 model predictions are favoured. The oldest horizon able to be reliably dated by CRS2 occurs at 89 cm (91 ±3 years).

The sediment accumulation rate history for Lake King determined from CRS2 ages is shown in Figure 9. Accumulation rates are highest in the first part of the 1900's. Another peak is seen in the late 1960's to early 1970's. On a multi-decadal time frame the sediment accumulation rates are 4.8 kg m^{-2} yr^{-1} for 1905-1940, 3.9 kg m^{-2} yr^{-1} for 1940 to 1975, and 3.3 kg m^{-2} yr^{-1} for 1975 to 2004. The long-term (100 year) accumulation rate is 3.65 ±0.17 kg m^{-2} yr^{-1} (Table 4).

Table 4. Parameters used in determining the chronologies of Lake Victoria and Lake King cores. $C(0)$ is required for the CIC chronology; A_{∞}^{Pb} is equivalent to $A(\infty)$, and is used for CRS applications. $r_{long\text{-}term}$ gives the long-term (100 year) accumulation rate for each core.

Site	$C(0)$ ($^{210}Pb_{ex}$)	A_{∞}^{Pb} (Bq m^{-2})	A_{∞}^{Cs} (Bq m^{-2})	$r_{long\text{-}term}$ (kg m^{-2} yr^{-1})
Lake Victoria LV2	149 ±7	9610 ±240	1410 ±20	3.22 ±0.14
Lake King LK2	76.3 ±3.2	8670 ±200	572 ±11	3.65 ±0.17

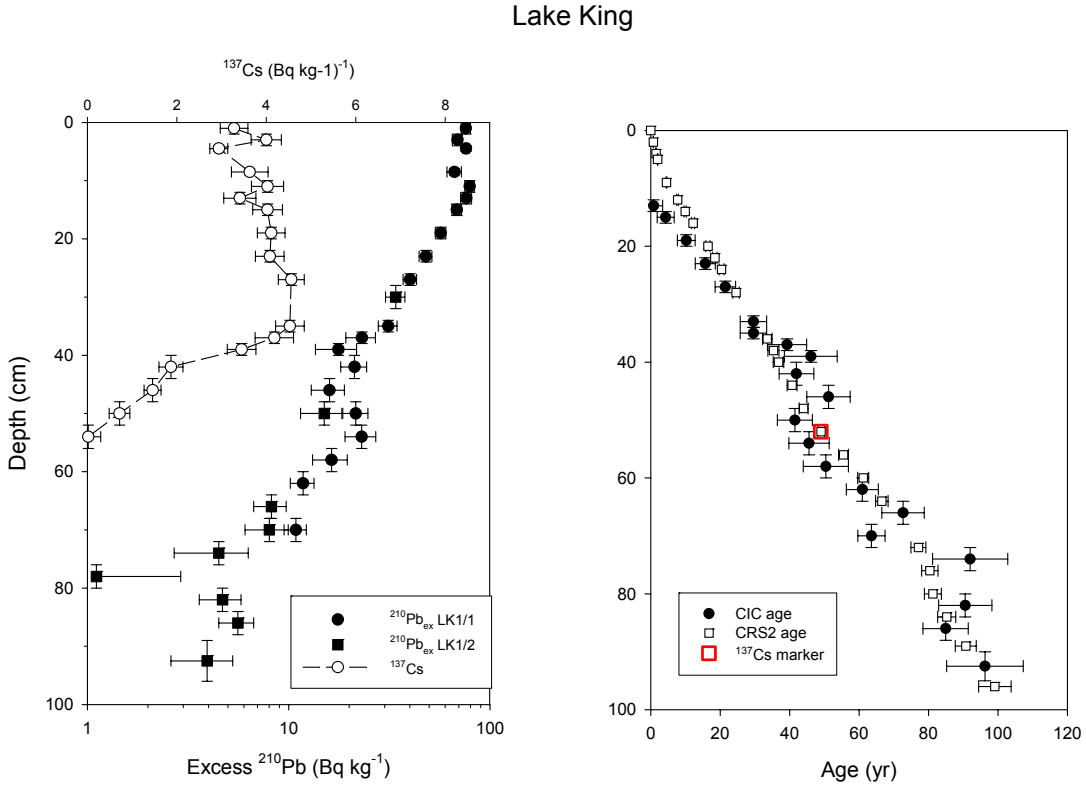

Figure 10. (Left) core profiles of $^{210}Pb_{ex}$ and ^{137}Cs for Lake King. (Right) chronologies determined using the various models (see text for details). The chronology given by the (calibrated) CRS2 model has been adopted.

3.3.3. Optical dating of Lake Victoria and Lake King sediment

The sediment from Lakes Victoria and King did not produce adequate numbers of single-grain D_e values to enable accurate estimation of a burial dose. The three samples produced only two, four and seven single grain D_e values (Table 3). However, despite the high relative uncertainties (>100% in many cases) for D_e values of individual grains, it is possible to determine a maximum possible for all the sediment samples. For the deepest samples (depth >120 cm) the maximum age is 150 years, and for the 90-96 cm from Lake King a maximum age of 100 year is determined. These ages are consistent with the ^{210}Pb-^{137}Cs chronologies.

4. DISCUSSION

4.1. Lake Wellington

The range in sediment load calculated for Lake Wellington using the sediment core profiles at LW2 and LW3 (110-172 kt yr^{-1}) encompasses many of the estimates made in recent studies. Using monitoring data and catchment modelling Grayson et al. (2001) and Grayson and Argent (2002) estimated catchment loads of 151-160 kt yr^{-1}. As noted above the load estimates calculated here assume an even distribution of sediment throughout the Lake. The Lake is shallow (maximum depth ~3.5 m) with a relatively flat base, so this is probably a reasonable assumption. However, if

sediment is being focussed towards the centre of the Lake (in the region of the coring sites) then our load estimates will be too high. Another caveat concerns export of sediment from Lake Wellington, discussed above. If this process is significant our estimate of the depositional load in Lake Wellington will underestimate the catchment load delivered by West Gippsland rivers.

The change in the geochemical composition of sediment corresponding to the last 50-70 years or longer suggests that new sources of sediment have been accessed, or else the hydrology of the river has changed. Higher concentrations of SiO_2 may indicate that more fine sand (quartz) has been delivered in recent times. Because sand particles are generally coarser and denser than silt and clay-sized particles an increase in sand may indicate a more energetic flow regime. Certainly the coarse-grained nature of bed sediment in much of the river channels in Gippsland indicates that large volumes of sand are moving through the river network. The elements Zr and Ti are associated with the dense minerals zircon and ilmenite, which along with quartz, suggest a heavy detrital component. Thus an increase in ZrO_2 and TiO_2 is also indicative of a more energetic flow regime.

The Fe oxide profile also suggests a changing sediment source. The decrease in Fe_2O_3 above 22 cm is greater than would be expected from dilution with Fe-free sand (SiO_2). High levels of P (expressed as P_2O_5) in the upper 22 cm may be due to primary production in the overlying water column, although the poor correlation with LOI (organic matter) suggests primary production may not be entirely responsible. To test the alternative explanation, i.e. P enrichment from anthropogenic sources in the Lake Wellington catchment, would require a more sensitive analysis of organic carbon than that given by LOI.

4.2. Lake Victoria and Lake King

The medium-term (last 50 years) accumulation rates for Lake Victoria and Lake King, although different on a linear depth scale basis (1.7 and 1.0 cm yr^{-1} respectively), are very similar on a cumulative mass basis. The higher vertical rates in Lake Victoria are clearly due to the higher porosity of the LV2 sediment (Figure 4). It is instructive to compare the $^{210}Pb_{ex}$ and ^{137}Cs depth profiles of the two cores with depth presented as cumulative mass rather than a length scale (Figure 11). Apart from the first few cm of the Lake Victoria core, the $^{210}Pb_{ex}$ profiles show a good correlation. The horizon of first appearance of ^{137}Cs also compares well. Not surprisingly their long-term accumulation rates ($r_{longterm}$ in Table 4) are similar.

It is interesting to note the historical pattern of accumulation shown in Figure 9. The rate of sediment accumulation in Lake King in the period 1915-1940 is 2.5 times higher than Lake Victoria. This period of elevated accumulation in Lake King preceded an increase in Lake Victoria accumulation, which accelerated from 1940 through to the mid-1950's. A similar, although less significant trend is seen in the late 1960's to mid-1970's in Lake King, and the 1980's in Lake Victoria. As discussed below, the high activities of $^{210}Pb_{ex}$ at the surface of Lake Victoria may reflect re-distribution of sediment originally deposited elsewhere in the Gippsland Lakes. The patterns in Figure 9 may therefore indicate that Lake King is the initial deposition site for sediment delivered from the East Gippsland catchment, but a proportion of this sediment is slowly redistributed into Lake Victoria on a time scale of years to decades.

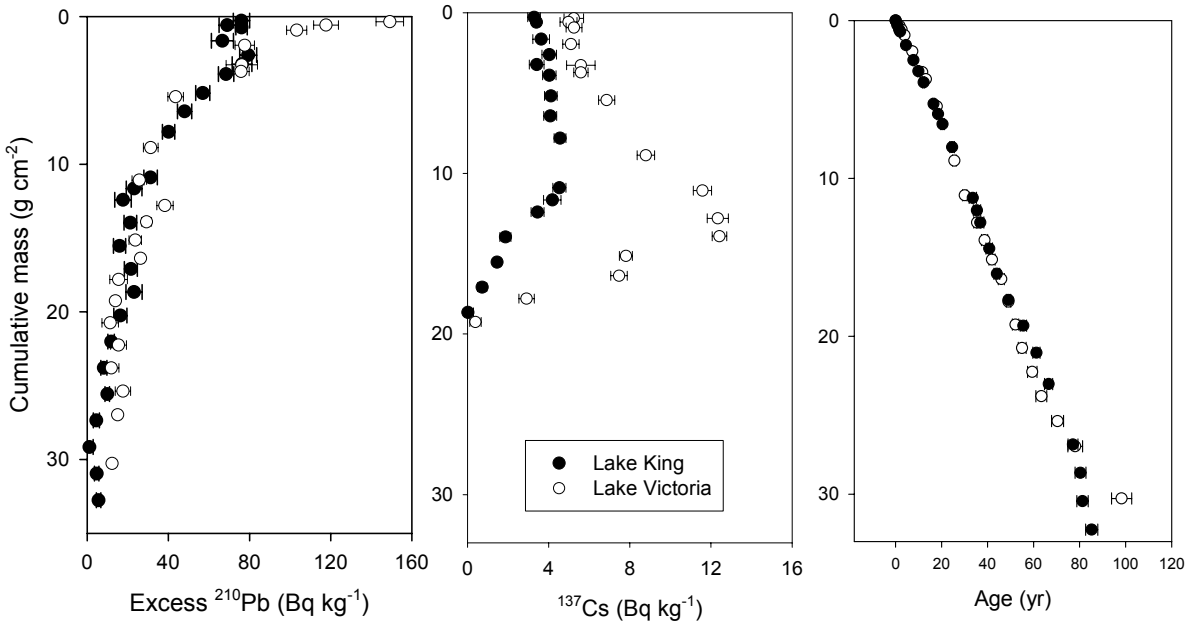

Figure 11. Comparison of the Lake Victoria and Lake King profiles and chronologies. Depth is expressed as cumulative mass.

The ^{137}Cs concentrations and inventories in Lake Victoria sediment are significantly higher than Lake King and Lake Wellington. This observation indicates that the deep regions of Lake Victoria are the final deposition site for much of the ^{137}Cs entering the Lake system and probably reflects the deep and relatively sheltered nature of Lake Victoria. A similar pattern of sediment and fallout nuclide focussing has been observed in the nearby Western Port embayment (Hancock et al., 2001). The resuspension and transport processes most likely responsible for the redistribution of sediment in the Lakes would favour the movement of smallest (finest) sediment particles. These particles would preferentially scavenge and deposit dissolved ^{137}Cs delivered directly from the atmosphere and would lead to a highly porous, high ^{137}Cs activity sediment deposit, as is seen in core LV2.

As noted above for Lake Wellington, the transport and deposition of the more particle-reactive $^{210}Pb_{ex}$ is apparently different to ^{137}Cs, and indicates that ^{137}Cs inventories should not be used to quantify the spatial distribution of sediment in the Lakes. For example, the ^{137}Cs inventory of the Lake Victoria core is 2.4 times higher that of Lake King, yet their $^{210}Pb_{ex}$ inventories are very similar. Given the fact that Pb is known to be a better particle tracer than Cs, especially in saline water, it is therefore likely that $^{210}Pb_{ex}$ inventories are a better tracer of sediment fate in the Gippsland Lakes than ^{137}Cs.

Extrapolation of the mean long-term accumulation rates determined at LV2 and LK1 (~3.5 kg m^{-2} yr^{-1}) to the entire area of Lake King and Lake Victoria (17.3 x 10^7 m^2) gives a sediment load of 606 kt yr^{-1}. This estimate is a factor of almost 10 higher than previous estimates of sediment input from the Mitchell, Nicholson and Tambo rivers (Grayson et al., 2001, Grayson and Argent 2002), a comparison that is best explained by the focussing of sediment in the deep water regions of the lakes. Certainly the two core sites LV2 and LK1 were in the deepest water of both lakes (water

depth ~7 m), and the variability in depth in the eastern lakes is large. For example, at least 50% of the area of the King-Victoria system is shallower than 3 m and waters deeper than 5 m probably account for < 25% of the Lake area. Shallow water would allow ongoing resuspension of recently deposited sediment, with subsequent deposition in deeper water. It is therefore not considered possible to obtain realistic load estimates for the eastern Gippsland Lakes using the core profiles examined in this study. A larger study examining additional cores from a variety of depositional areas is required.

5. CONCLUSIONS

- Two core profiles in central and western Lake Wellington provide evidence for changing sediment composition over the last 100 years. This change may be related to the hydrology of the river and/or a changing sediment source.

- The upper 8-10cm of sediment in Lake Wellington is mixed, probably by bioturbation.

- Modelling of excess ^{210}Pb and ^{137}Cs profiles together with the construction of an excess ^{210}Pb budget indicates that the sediment load delivered to Lake Wellington lies in the range 110-190 kt yr^{-1}.

- Optical dating of deep sediment indicates that the sediment load to Lake Wellington prior to European settlement (200-5000 year BP) was 17 ±3 kt yr^{-1}, a depositional load 6-10 times lower than load estimates pertaining to the last few decades.

- A 90-100 year history is determined for Lake Victoria and Lake King. Mass accumulation at the two sites is approximately equal indicating that sediment entering Lake Victoria and Lake King is evenly distributed between the two lakes. This re-distribution process, involving transport of sediment from Lake King to Lake Victoria, appears to be occurring on a time scale of 10-20 years.

- On a time scale of a few years accumulation rates in Lakes King and Victoria have varied considerably in the past 100 years. However, when averaged over the last 60 years sediment accumulation has been relatively constant across both lakes. There is evidence that accumulation in Lake King was significantly higher than Lake Victoria in the first few decades of the 1900's.

- The ^{210}Pb and ^{137}Cs inventories of the cores in Lake Victoria and Lake King indicate sediment is focussed in the deeper regions of the eastern Lakes. Thus the sedimentation rate at the two deep water sites examined in this study (7 m water depth) cannot be used for the estimation of sediment loads.

- Sediment core inventories indicate that at least 35% of the ^{137}Cs entering Lake Wellington has been exported, probably to Lake Victoria. However the excess ^{210}Pb inventories do not show the same pattern and it is unlikely that the ^{137}Cs inventories reflect gross sediment transport and fate. The apparent difference in the behaviour of ^{137}Cs and ^{210}Pb probably reflects their different chemistries.

REFERENCES

Aitken M. J., 1998. An Introduction to Optical Dating. The Dating of Quaternary Sediments by the Use of Photon-stimulated Luminescence. Oxford University Press, Oxford, 267 pp.

Appleby, P.G. (2001). Chronostratigraphic techniques in recent sediments In: *Tracking Environmental Change Using Lake Sediments*, *Basin Analysis, Coring and Chronological Techniques* **vol. 1**, W.M. Last and J.P. Smol eds., Kluwer Academic Publishers, The Netherlands (2001).

Appleby, P.G. and Oldfield F. (1992). Application of lead-210 to sedimentation studies. In: *Uranium-series Disequilibrium: Applications to Earth, Marine and Environmental Sciences*, M. Ivanovich and R.S. Harmon eds., 731-778, Clarendon press, Oxford.

Grayson, R., Tan, K. S. and Western, A. (2001). Estimation of sediment and nutrient loads into the Gippsland Lakes. CEAH Report 2/01. Centre for Environmental Applied Hydrology, University of Melbourne.

Grayson, R. and Argent, R. (2002). A tool for investigating broad-scale nutrient and sediment sources from the catchments of the Gippsland Lakes. CEAH Report 1/02. Centre for Environmental Applied Hydrology, University of Melbourne.

Hancock, G.J., Olley, J.M. and Wallbrink, P J. (2001). Sediment transport and accumulation in Western Port. CSIRO Land and Water technical report 47/01.

Huntley D. J., Godfrey-Smith D. I. and Thewalt M. L. W., (1985). Optical dating of sediments. *Nature* **313**, 105-107.

Martin, P. and Hancock, G.J. (2004). Routine analysis of naturally occurring radionuclides in environmental samples by alpha-particle spectrometry. Supervising Scientist Report 180, Supervising Scientist, Darwin, N.T., Australia.

Mejdahl, V. (1979). Thermoluminescence dating: beta-dose attenuation in quartz grains. *Archaeometry* **21**, 61-72.

Murray A. S., Marten R., Johnston A., and Martin P. (1987) Analysis for naturally occurring radionuclides at environmental levels by gamma spectrometry. *Journal of Radioactive and Nuclear Chemistry*, **115,** 263-288.

Norrish, K., and Hutton J.T. (1969). An accurate X-ray spectrographic method for the analysis of a wide range of geological samples. *Geochimica et Cosmochimica Acta* **33**, 431-453.

Norrish, K., and Chappell B.W. (1977). X-ray fluorescence spectrometry. In 'Physical methods in determinative mineralogy', second edition, ed. J. Zussman (Academic Press: London), 201-272.

Olley, J.M., Pietsch, T. and Roberts R.G. (2004). Optical dating of Holocene sediments from a variety of geomorphic settings using single grains of quartz, *Geomorphology,* **60**, 337-358.

Reid, M. (1989). Palaeoecological changes at Lake Wellington, Gippsland Lakes, Victoria, during the late Holocene: A study of the development of a Coastal Lake ecosystem. Unpublished BSc Hons thesis, Department of Geography and Environmental Science, Monash University.

Robbins, J. A. (1978). Geochemical and geophysical applications of radioactive lead. In: *The Biogeochemistry of Lead in the Environment*, Part A, ed. J.O. Nriagu. pp 285-393, Elsevier Scientific, Amsterdam.

S. Stokes, Ingram, S., Aitken, M.J., Sirocko, F., Anderson, R. and Leuschner, D. (2003). Alternative chronologies for Late Quaternary (Last Interglacial–Holocene) deep sea sediment via optical dating of silt-size quartz, *Quaternary Science Reviews* **22**, 925–941.

Turekian, K.K., Nozaki, Y. and Benninger, L.K. (1977). Geochemistry of atmospheric radon and radon products. *Annual Review of Earth and Planetary Science*s, **5**, 227-255.

H. Yoshida, Roberts, R.G., Olley, J.M., Laslett, G.M. and Galbraith, R.F. (2000). Extending the age range of optical dating using single 'supergrains' of quartz, *Radiation Measurements* **32**, 439–446.

Wallbrink, P.J. and Murray, A.S. (1996). Determining soil loss using the inventory ratio of excess ^{210}Pb to ^{137}Cs. *Soil Science of America Journal*, **60**, 1201-1208.

Webster, I.T., Parslow, J.S., Grayson, R.B., Molloy, R. P., Andrewartha, J, Sakov, P., Kim, S.T., Walker, S.J. and Wallace, B.B. (2001). Gippsland Lakes environmental study assessing options for improving water quality and ecological function. Final Report, November 2001, CSIRO, Glen Osmond, SA, Australia.

APPENDICES

Depth (cm)	% water	Porosity	Cum. dry mass (g cm^{-2})	^{137}Cs (Bq kg^{-1})	$^{210}Pb_{ex}$ (Bq kg^{-1})
LW2/1					
0-1	71.4	0.852	0.341	1.97 0.26	50.0 3.1
1-2	60.5	0.779	0.850		
2-3	62.9	0.796	1.319		
3-4	62.1	0.791	1.800	3.56 0.3	48.7 3.6
4-5	61.7	0.788	2.289		
5-6	61.5	0.786	2.782	2.93 0.33	43.1 3.8
6-7	61.2	0.784	3.278		
7-8	60.5	0.779	3.787	3.68 0.38	38.2 4.4
8-9	59.5	0.772	4.312		
9-10	58.9	0.767	4.848	3.94 0.47	21.8 5.3
10-11	58.8	0.766	5.385		
11-12	58.8	0.766	5.922	2.89 0.21	17.6 2.3
12-13	58.1	0.761	6.471		
13-14	57.5	0.757	7.030	2.88 0.29	13.6 3.3
14-15	56.0	0.745	7.616		
15-16	57.6	0.758	8.173		
16-18	57.4	0.756	9.294	2.1 0.21	10.5 2.4
18-20	59.7	0.773	10.338		
20-22	62.9	0.796	11.276	1.33 0.25	6.2 1.7
22-24	68.1	0.831	12.054	0.53 0.28	0.5 1.2
24-26	69.3	0.838	12.798	-0.65 0.24	1.9 3.6
26-28	70.2	0.844	13.514	-0.23 0.23	2.8 2.9
28-30	69.1	0.837	14.263		
LW3/1					
0-2	66.0	0.817	0.840	2.76 0.28	43.0 4.2
2-4	68.7	0.835	1.601		
4-6	65.9	0.816	2.446	3.1 0.3	49.9 4.3
6-8	62.8	0.795	3.387	3.69 0.31	47.8 4.1
8-10	62.0	0.790	4.355	3.51 0.26	42.3 3.7
10-12	62.3	0.792	5.311		
12-14	62.7	0.795	6.255	2.89 0.25	31.9 3.7
14-16	62.2	0.791	7.218		
16-18	61.5	0.786	8.203	2.77 0.27	16.5 3.8
18-20	60.4	0.778	9.224		
20-22	62.1	0.790	10.190	0.78 0.21	9.8 1.6
22-24	59.6	0.772	11.237	0.53 0.28	10.3 1.8
24-26	65.3	0.813	12.099	-0.15 0.25	6.9 3.9
26-28	65.2	0.812	12.965		1.3 1.6
28-30	67.6	0.827	13.759	-0.28 0.2	0.1 1.5
30-32	68.2	0.831	14.536	0.12 0.33	4.3 4.5

Table A1. Lake Wellington core data. Uncertainties are given in the minor font and correspond to ±1 s.e.

Depth (cm)	% water	Porosity	Cum. dry mass (g cm^{-2})	^{137}Cs (Bq kg^{-1})	^{210}Pb$_{ex}$ (Bq kg^{-1})	CIC age (yr)	CRS age (yr)	CRS2 age (yr)
Lake Victoria								
0-2	87.6	0.942	0.267	5.24 0.48	149.1 6.8	2.3 1.8	0.0 0.0	0.0 0.0
2-4	82.8	0.917	0.647	4.98 0.42	117.7 6.1	9.9 1.9	1.6 0.08	1.7 0.1
4-6	82.4	0.915	1.038	5.25 0.39	103.3 5.0	14.1 1.8	2.5 0.1	2.6 0.1
6-8	82.1	0.914	1.436				3.8 0.1	3.9 0.1
8-10	82.7	0.917	1.820					
10-12	82.3	0.915	2.213	5.1 0.4	77.6 4.8	23.3 2.2		
12-14	81.3	0.909	2.632				7.0 0.2	7.2 0.2
14-16	81.0	0.907	3.058					
16-18	84.1	0.924	3.408					
18-20	81.3	0.909	3.828	5.59 0.7	76.2 7.7	23.9 3.4		
20-22	80.0	0.902	4.279	5.59 0.35	75.8 4.0	24.1 2.0	11.2 0.4	11.6 0.4
22-24	82.8	0.917	4.661				12.7 0.4	13.2 0.4
24-26	82.8	0.917	5.042					
26-28	81.1	0.908	5.465					
28-32	79.0	0.896	6.419	6.86 0.4	43.6 3.8	41.9 3.0		
32-36	75.6	0.877	7.553				17.3 0.6	17.9 0.5
36-40	74.2	0.869	8.761					
40-44	75.8	0.878	9.884	8.79 0.43	31.3 3.6	52.5 3.9		
44-48	76.1	0.880	10.988				24.5 0.8	25.5 0.8
48-52	77.0	0.885	12.047	11.58 0.45	25.7 3.6	58.9 4.6		
52-56	79.9	0.901	12.955				28.8 1.0	30.0 0.9
56-60	79.6	0.900	13.879	12.34 0.52	38.3 4.0	46.0 3.5		
60-64	75.5	0.876	15.018	12.42 0.36	29.2 2.5	54.7 2.9	33.8 1.2	35.4 1.4
64-68	73.3	0.863	16.275	7.81 0.32	23.7 3.0	61.5 4.2	36.8 1.3	38.7 1.4
68-72	70.8	0.848	17.672	7.47 0.41	26.3 1.9	58.1 2.5	39.7 1.5	41.9 1.3
72-76	70.3	0.845	19.098	2.91 0.38	15.5 4.4	75.2 9.1	43.4 1.7	46.0 1.3
76-80	69.8	0.842	20.553	0.39 0.28	13.9 1.6	78.7 3.9	46.2 1.8	49.1 1.0
80-84	69.3	0.839	22.037	0.33 0.26	11.3 4.1	85.2 11.6	48.9 2.0	52.2 1.4
84-88	68.8	0.836	23.550	0.13 0.27	15.4 3.9	75.3 8.2	51.4 2.1	55.0 1.7
88-92	68.3	0.832	25.093	-0.39 0.26	11.9 3.7	83.6 10.1	55.2 2.2	59.4 2.0
92-96	67.8	0.829	26.666	-0.04 0.23	17.6 3.8	71.0 6.9	58.5 2.4	63.4 2.4
96-100	67.3	0.826	28.269	0.14 0.26	15.0 1.5	76.2 3.4	64.3 2.6	70.4 2.6
100-104	66.8	0.823	29.902				70.4 3.2	78.1 3.2
104-108	66.3	0.819	31.565		12.2 1.8	82.8 4.7		
108-112	65.8	0.816	33.259				84.6 4.2	98.3 4.4

Table A2. Summary of Lake Victoria core data and chronologies. CRS ages correspond to the upper horizon of each depth interval. Uncertainties (minor font) correspond to ±1 s.e.

Depth (cm)	% water	Porosity	Cum. dry mass (g cm^{-2})	^{137}Cs (Bq kg^{-1})		^{210}Pb$_{ex}$ (Bq kg^{-1})		CIC age (yr)		CRS age (yr)		CRS2 age (yr)	
Lake King													
0-2	87.0	0.939	0.281	3.28	0.31	76.0	4.0			0.0	0.00	0.0	0.0
2-4	86.0	0.934	0.585	4.72	0.34	69.0	4.0			0.8	0.02	0.8	0.0
4-5	85.5	0.931	0.743	2.94	0.2	76.1	2.8			1.6	0.06	1.5	0.1
5-6	86.3	0.935	0.891							2.0	0.03	2.0	0.1
6-7	81.7	0.911	1.095										
7-8	78.3	0.893	1.341										
8-9	74.0	0.867	1.646	3.63	0.41	66.6	5.4						
9-10	71.9	0.855	1.981							4.7	0.11	4.5	0.2
10-12	73.2	0.863	2.613	4.03	0.36	79.3	4.2						
12-14	73.9	0.867	3.226	3.41	0.36	76.3	4.8	0.8	2.6	8.0	0.2	7.8	0.3
14-16	71.8	0.854	3.897	4.03	0.33	68.5	3.8	4.3	2.4	10.3	0.3	9.9	0.3
16-18	72.4	0.858	4.550							12.7	0.4	12.2	0.4
18-20	73.1	0.862	5.184	4.11	0.31	57.0	3.4	10.2	2.5				
20-22	73.6	0.865	5.805							17.2	0.6	16.5	0.6
22-24	73.5	0.865	6.427	4.08	0.32	48.0	3.5	15.7	2.9	19.3	0.7	18.5	0.7
24-26	71.7	0.853	7.102							21.3	0.8	20.4	0.8
26-28	70.3	0.845	7.815	4.56	0.29	40.1	3.1	21.5	3.0				
28-30	69.5	0.840	8.552							25.7	1.0	24.6	1.0
30-32	67.4	0.826	9.351										
32-34	68.3	0.832	10.124										
34-36	68.2	0.831	10.900	4.53	0.32	31.2	3.3	29.6	3.8				
36-38	68.9	0.836	11.654	4.18	0.43	23.1	3.9	39.3	5.6	35.5	1.6	33.6	1.6
38-40	68.8	0.835	12.411	3.45	0.32	17.7	4.1	46.1	7.6	37.4	1.7	35.4	1.5
40-44	68.2	0.831	13.963	1.87	0.27	21.3	3.1	42.0	5.0	39.0	1.8	36.8	1.5
44-48	67.8	0.829	15.535	1.46	0.19	16.0	3.0	51.2	6.2	43.4	2.1	40.7	1.4
48-52	68.1	0.831	17.092	0.72	0.23	21.6	3.2	41.5	5.0	47.1	2.4	44.0	1.2
52-56	68.0	0.830	18.656	0.02	0.28	23.1	4.0	45.6	5.8	52.9	2.9	49.1	1.0
56-60	67.4	0.826	20.255	0.35	0.24	16.4	3.2	50.4	6.5	60.5	3.7	55.5	1.4
60-64	64.8	0.809	22.013	-0.32	0.25	11.8	1.6	61.0	4.6	67.5	4.4	61.2	1.5
64-68	64.5	0.807	23.790	-0.01	0.24	8.2	1.5	72.7	6.1	74.3	5.3	66.6	1.7
68-72	64.5	0.807	25.566	0.34	0.23	9.9	1.1	63.6	3.9				
72-76	64.3	0.806	27.355	-0.07	0.15	4.5	1.5	92.0	10.8	89.1	8.4	77.1	2.0
76-80	64.1		29.157	0.01	0.17	1.1	1.8			94.1	9.8	80.4	2.2
80-84	64.1	0.804	30.958	-0.24	0.13	4.7	1.1	90.6	7.7	95.5	10.1	81.3	2.3
84-88	64.1		32.760	-0.14	0.12	5.6	1.1	84.9	6.5	102.2	12.2	85.3	2.5
89-96	64.1	0.804	35.912	-0.42	0.25	3.9	1.3	96.3	11.0	112.4	16.9	90.7	2.9
116-120	64.1	0.800	37.714	-0.09	0.14								

Table A3. Summary of Lake King core data and chronologies. CRS ages correspond to the upper horizon of each depth interval. Uncertainties (minor font) correspond to ±1 s.e.

LW2/1

Depth	SiO_2	Al_2O_3	MgO	Fe_2O_3	CaO	Na_2O	K_2O	TiO_2	P_2O_5	MnO	SO_3	ZnO	CuO	SrO	ZrO_2	NiO	Rb_2O	BaO	V_2O_5	Cr_2O_3	La_2O_3	CeO_2	PbO	Y_2O_3	Ga_2O_3	ThO_2	As_2O_5
cm	%	%	%	%	%	%	%	%	%	%	%	ppm	ppm	ppm	ppm	ppm	ppm	ppm	ppm	ppm	ppm	ppm	ppm	ppm	ppm	ppm	ppm
0-1	65.8	13.0	1.00	4.97	1.50	0.72	1.88	0.92	0.16	0.09	0.34	110	9	120	365	36	140	413	158	148	63	127	28	56	31	30	30
2-4	64.6	14.9	1.04	5.25	0.26	0.54	2.09	0.95	0.14	0.04	0.45	117	9	73	282	55	157	434	191	170	47	139	29	58	35	35	28
5-6	65.5	14.6	1.09	5.26	0.24	0.51	2.08	0.96	0.14	0.05	0.49	126	6	72	300	43	160	412	177	157	49	133	25	59	34	31	30
7-8	65.8	14.6	1.06	5.36	0.25	0.58	2.09	0.95	0.14	0.05	0.51	109	13	66	281	43	160	417	184	157	55	148	29	55	33	32	35
9-10	65.7	14.2	1.06	5.27	0.21	0.59	2.03	0.91	0.11	0.04	0.58	111	9	66	282	39	154	425	186	149	56	134	31	58	31	34	39
11-12	66.1	14.3	1.03	5.19	0.21	0.53	2.03	0.91	0.11	0.04	0.70	103	5	62	285	38	154	425	198	162	63	134	28	60	35	35	36
12-14	66.5	14.3	1.03	5.18	0.21	0.48	2.04	0.90	0.11	0.04	0.74	106	5	60	287	44	152	446	174	158	56	138	27	57	33	35	37
16-18	66.0	14.5	1.07	5.04	0.21	0.48	2.17	0.91	0.11	0.04	0.73	109	9	65	283	43	160	453	181	155	47	147	29	62	32	34	36
20-22	65.8	14.2	1.04	5.52	0.21	0.63	1.89	0.83	0.10	0.04	0.96	104	12	61	250	42	143	422	166	161	56	130	25	53	33	27	35
22-24	56.6	17.4	1.31	8.24	0.21	0.45	2.01	0.77	0.09	0.06	1.88	117	12	57	197	45	162	419	226	177	47	121	30	56	38	34	45
24-26	54.2	18.1	1.39	9.17	0.21	0.42	2.03	0.76	0.09	0.06	2.11	116	10	60	182	50	164	412	221	180	46	120	27	50	40	37	35
28-30	53.9	18.1	1.39	9.10	0.21	0.42	2.06	0.77	0.08	0.07	2.26	118	9	62	185	50	166	430	222	180	58	118	25	51	41	33	35
34-36	53.7	18.9	1.45	8.71	0.22	0.40	2.28	0.77	0.08	0.07	1.94	125	9	67	193	52	185	485	240	178	59	124	31	53	42	36	34
40-44	54.8	17.7	1.20	8.97	0.16	0.38	2.00	0.75	0.08	0.07	5.01	106	11	53	181	42	163	386	215	174	42	122	25	45	38	30	42
48-52	54.3	18.6	1.39	8.21	0.23	0.39	2.05	0.75	0.07	0.09	3.81	113	10	64	172	57	167	371	225	178	42	126	30	52	40	33	34
56-60	53.7	18.7	1.29	8.52	0.18	0.42	1.99	0.73	0.08	0.07	4.41	107	18	57	171	47	168	398	219	181	43	118	28	47	41	34	28
60-64	54.9	18.5	1.36	8.01	0.22	0.42	2.03	0.74	0.08	0.07	3.79	108	16	60	160	56	167	418	214	170	53	120	29	50	41	30	33

Table A4. Lake Wellington (LW2) XRF data.

LV2

Depth	SiO_2	Al_2O_3	MgO	Fe_2O_3	CaO	Na_2O	K_2O	TiO_2	P_2O_5	MnO	SO_3	ZnO	CuO	SrO	ZrO_2	NiO	Rb_2O	BaO	V_2O_5	Cr_2O_3	La_2O_3	CeO_2	PbO	Y_2O_3	Ga_2O_3	ThO_2	As_2O_5	LOI
cm	%	%	%	%	%	%	%	%	%	%	%	ppm	ppm	ppm	ppm	ppm	ppm	ppm	ppm	ppm	ppm	ppm	ppm	ppm	ppm	ppm	ppm	%
0-2	47.5	15.0	1.53	5.19	1.48	3.20	2.15	0.64	0.29	0.03	0.78	138	17	126	187	51	173	394	245	180	59	89	20	45	27	22	9	19.6
2-4	48.0	15.6	1.61	5.61	1.00	3.24	2.23	0.65	0.21	0.04	0.86	133	12	118	204	39	174	390	243	143	60	92	25	62	30	22	9	18.1
4-6	50.0	17.0	1.62	6.12	0.51	2.09	2.38	0.70	0.19	0.05	0.93	129	8	101	180	51	188	418	241	171	48	96	23	57	32	20	10	16.7
10-12	49.8	18.7	1.80	6.08	0.51	2.66	2.57	0.70	0.15	0.05	1.19	127	7	102	173	46	200	467	235	167	50	106	31	45	33	22	11	13.6
18-20	49.2	20.3	1.93	6.73	0.77	1.62	2.70	0.73	0.15	0.04	1.21	147	3	107	177	51	217	480	244	181	55	105	35	39	37	20	8	13.4
22-26	50.6	18.4	1.81	7.05	0.73	0.89	2.53	0.67	0.17	0.04	1.60	138	11	114	174	51	199	413	258	177	50	113	41	31	43	39	26	14.9
28-32	51.8	20.6	1.94	6.68	0.44	1.20	2.80	0.73	0.14	0.05	1.26	136	2	95	163	44	225	497	246	187	45	116	33	32	38	16	19	11.4
40-44	50.8	20.8	2.07	6.90	0.92	1.11	2.90	0.76	0.14	0.04	1.36	138	8	118	189	71	236	507	241	242	39	109	35	36	36	17	17	11.4
48-52	50.0	20.0	2.18	6.58	1.77	1.20	2.90	0.67	0.16	0.04	1.23	130	9	149	167	47	226	481	254	229	43	114	27	33	35	19	18	12.4
56-60	52.3	19.3	2.33	6.96	0.62	0.94	2.70	0.77	0.16	0.07	1.41	129	5	101	173	52	209	495	242	172	38	111	31	43	35	18	14	11.8
60-64	51.0	20.4	2.12	7.07	0.91	0.82	2.71	0.75	0.17	0.05	2.63	131	29	105	179	57	217	466	256	182	39	117	41	27	48	39	44	10.8
64-68	51.1	20.7	2.06	7.25	0.51	0.77	2.75	0.73	0.17	0.04	3.49	133	30	100	167	57	219	461	274	178	50	119	34	28	44	37	50	9.9
68-72	51.1	21.2	2.01	7.30	0.46	0.90	2.91	0.75	0.15	0.03	1.41	143	24	99	169	56	227	519	253	193	45	98	26	37	35	15	31	11.2
60-64	50.5	20.7	1.92	7.43	0.59	0.82	2.77	0.74	0.16	0.04	1.42	137	21	100	174	54	215	492	272	190	42	107	37	23	45	35	43	12.4
64-68	50.6	21.7	1.95	7.09	0.62	0.82	2.94	0.76	0.17	0.03	1.25	140	23	104	176	56	229	507	273	190	41	102	36	23	47	39	38	11.6
68-72	50.0	21.4	1.90	7.59	0.81	0.88	2.91	0.74	0.17	0.03	1.56	132	8	115	190	56	236	461	250	195	48	116	33	25	48	38	38	11.4
72-76	51.2	21.8	1.82	7.39	0.78	0.79	3.02	0.82	0.19	0.03	0.98	133	17	110	180	53	234	572	254	186	53	122	34	29	48	36	30	10.6
76-80	52.5	21.4	1.79	7.23	0.49	0.77	3.08	0.84	0.18	0.03	0.74	135	13	99	178	48	238	542	264	184	52	126	34	32	46	37	33	10.5
80-84	51.3	22.1	1.89	7.13	0.75	0.58	3.16	0.73	0.18	0.03	1.95	135	26	111	164	58	254	530	257	183	53	115	37	24	48	37	51	9.8
84-88	50.8	20.3	1.97	7.18	0.65	0.86	2.83	0.70	0.17	0.04	2.80	126	20	100	156	44	221	466	227	169	47	110	39	32	41	36	63	11.2
88-92	51.2	19.7	1.90	7.08	1.30	0.82	2.81	0.71	0.16	0.04	2.93	123	16	122	163	51	221	500	236	170	54	105	36	31	41	34	44	10.8
92-96	51.4	20.2	1.96	6.91	1.04	0.85	2.90	0.71	0.16	0.05	2.92	126	17	112	154	43	232	468	232	175	58	120	33	25	43	36	40	10.4

Table A5. Lake Victoria (LV2) XRF data.

LK1

Depth	SiO_2	Al_2O_3	MgO	Fe_2O_3	CaO	Na_2O	K_2O	TiO_2	P_2O_5	MnO	SO_3	ZnO	CuO	SrO	ZrO_2	NiO	Rb_2O	BaO	V_2O_5	Cr_2O_3	La_2O_3	CeO_2	PbO	Y_2O_3	Ga_2O_3	ThO_2	As_2O_5	LOI
cm	%	%	%	%	%	%	%	%	%	%	%	ppm	ppm	ppm	ppm	ppm	ppm	ppm	ppm	ppm	ppm	ppm	ppm	ppm	ppm	ppm	ppm	%
0-1	50.3	15.3	1.97	5.45	2.33	2.79	2.50	0.64	0.20	0.04	3.26	137	33	167	208	182	378	190	146	63	115	36	49	43	29	25	35	13.0
3-5	50.9	15.6	1.78	5.66	3.54	1.85	2.57	0.67	0.15	0.04	3.47	133	32	201	232	184	382	186	145	66	121	37	46	43	29	24	38	12.5
6-8	50.1	15.7	1.72	5.87	3.41	1.51	2.46	0.64	0.15	0.04	4.02	131	39	199	198	186	384	194	132	53	122	39	47	36	29	21	39	13.4
8-10	49.6	16.2	1.76	6.07	2.94	1.47	2.47	0.63	0.16	0.04	4.24	141	26	185	180	190	384	205	142	46	119	34	47	39	29	20	40	13.4
10-12	50.5	16.6	1.80	6.20	2.50	1.25	2.56	0.66	0.15	0.05	3.94	140	32	171	186	189	388	199	133	47	117	39	54	45	25	21	37	12.9
14-16	51.5	16.5	1.86	6.20	1.95	1.46	2.42	0.65	0.15	0.04	4.08	119	29	164	192	184	378	191	140	47	118	35	46	30	31	23	34	12.2
18-20	50.8	16.4	1.89	6.17	2.38	1.36	2.40	0.64	0.14	0.04	3.92	115	26	175	168	180	378	181	149	40	115	30	46	31	28	19	36	12.9
22-24	50.3	16.4	1.82	6.11	3.48	1.16	2.39	0.63	0.14	0.03	3.95	120	25	222	187	177	369	189	138	42	116	31	40	42	30	21	41	12.9
28-32	50.1	16.6	1.78	6.19	3.70	1.11	2.43	0.63	0.13	0.03	3.98	118	26	222	191	184	381	191	144	67	104	35	48	38	31	20	41	12.7
36-34	50.5	18.4	1.90	6.72	1.98	1.22	2.61	0.68	0.15	0.03	4.02	129	30	167	184	200	365	212	152	49	119	39	48	40	32	19	49	11.0
44-48	50.6	18.6	1.92	6.69	2.17	1.03	2.66	0.70	0.15	0.04	3.35	126	25	172	191	204	383	208	146	46	128	41	45	26	32	18	48	11.4
48-52	51.3	17.7	1.87	6.48	2.14	1.07	2.58	0.69	0.14	0.04	3.73	129	27	173	180	195	371	207	142	40	128	35	48	37	30	21	49	11.7
52-56	51.8	17.5	1.94	6.39	2.19	1.11	2.63	0.69	0.14	0.04	3.54	130	28	169	173	198	362	194	143	49	134	39	44	54	30	16	45	11.4
56-60	51.8	18.4	1.98	6.73	1.49	1.09	2.76	0.72	0.14	0.04	3.30	142	26	158	188	206	397	213	142	49	126	43	51	36	34	21	50	10.9
64-68	51.1	19.6	1.95	6.99	1.85	0.96	2.88	0.76	0.15	0.04	2.93	143	27	158	166	217	409	217	150	54	123	41	46	28	32	21	48	10.3

Table A6. Lake King (LK1) XRF data.